Available online at www.sciencedirect.com
ScienceDirect
Coordination Chemistry Reviews 251 (2007) 1987–2016
COORDINATION CHEMISTRY REVIEWS
www.elsevier.com/locate/ccr

Review

Coordination and supramolecular network entanglements of organodisulfonates

Veneta Videnova-Adrabinska *

Department of Chemistry, Wroclaw University of Technology, 23 Wybrzeże Wyspiańskiego Street, 50-370 Wroclaw, Poland

Received 7 December 2006; accepted 30 March 2007
Available online 5 April 2007

Contents

1. Introduction 1987
2. General properties of sulfonic acids 1988
3. Hydrogen bond and coordination abilities of the sulfonate group 1988
4. Classification of sulfonic compounds 1989
5. Methodology 1990
6. Solvated metal ion disulfonates 1990
7. Delineation of the coordination frameworks of transition metal ion complexes 1993
   7.1. Isolated coordination units 1993
   7.2. One-dimensional coordination networks 1993
   7.3. Two-dimensional coordination networks 2003
   7.4. Three-dimensional coordination networks 2005
8. Group 2 (earth alkaline) metal ion complexes 2007
9. Summary and conclusions 2014
   Acknowledgement 2014
   References 2015

Abstract

The infinite solid state architectures of variable organodisulfonate coordination complexes, retrieved from CSD v. 5.27, have been analyzed. The extended metal-organic frameworks (MOF) of 90 compounds are discussed with respect to binding preferences and repeating structural and linking motifs, leading to coordination polymerization and/or supramolecular self-assembly. A disentanglement method is applied in order to gain insight into the ordered periodic arrangement and understand the structure-controlling factors, amenable for that organization. Such factors as coordination predisposition and geometrical preferences of the metal ion are particularly addressed. The functionality of the disulfonate ligands is considered with respect to the topology and binding abilities of the coordinating sites, from one side, and the nature, symmetry and the additional substituent(s) of the organic spacer, from the other side. A graph-set notation, similar to that used in hydrogen bonded systems, is proposed for identification of the structural and linking motifs, observed in the extended solids of the studied compounds.

Keywords: Organodisulfonates; Transition metal; Alkaline earth metal; Molecular organization; Metal-organic framework; Supramolecular network; Hydrogen bond; Disentanglement method; Graph-set

1. Introduction

Organization on both the molecular and supramolecular level is governed by the same fundamental physical force (the electromagnetic repulsion and attraction), which dominates on the whole scale of 10^{-10} to 10^{-6} m. Roughly 100 elements,

* Tel.: +48 71 3203266; fax: +48 71 3204360.
E-mail address: veneta@pwr.wroc.pl.

0010-8545/$ – see front matter © 2007 Elsevier B.V. All rights reserved.
doi:10.1016/j.ccr.2007.03.018

with unique electronic system of their atoms, account for the wealthy molecular world, and therefore, account for the steadily growing realm of sophisticated supramolecular systems and novel materials. However, the ordered information for structural organization on each level is decoded on its sublevel. The chemical properties of the molecule result from the combination of atoms and covalent bonds between them and the information for bond formation is carried by the individual atoms, that share their electrons. On the other hand the ordered information for molecular recognition and organization is deciphered in the structure of molecules themselves. According to the supramolecular conception the intermolecular interactions are considered as (bonding) connections between molecules [1]. So, it is reasonable that the synthetic and research efforts during the last two decades have moved from the traditional organic, inorganic and organometallic chemistry to supramolecular chemistry and focus on problems of (high level) molecular organization. The collective properties of well defined molecular assemblies have been compared with those of the individual components and addressed with respect to the structural relationships [2]. Nowadays the supramolecular paradigm is particularly shifting towards controlling the periodical distribution of noncovalent bonding and constructing ordered networks. In this context the crystal is reasonably considered as a "supermolecule par excellence" [3]. Variable approaches, targeted into reliable high-dimensional arrangement of molecular/ionic building blocks with predictable final architecture, are pursued by different research groups. Despite the none-questionable progress made in this direction [4,5], there are still white areas and black points. Managing the collective interplay and the periodical distribution of weak (non-specific) interactions is indispensable for directing the network entanglement. Such problems as understanding the nuclei formation and predicting the final outcome of the crystallization process, control over the supramolecular isomorphs and crystalline polymorphs continue to be challenging.

An useful way for gaining insight into the principles governing the ordered molecular organization, is to analyse a large number of representative crystal structures using disentanglement methods [6–9]. The present paper studies the coordination and supramolecular chemistry of disulfonic acids, with respect to their solid state arrangement. There is no systematic study of the extended metal-organic frameworks (MOF) of organodisulfonates with respect to the binding preferences of the sulfonic group, and especially, of the repeated structural and linking motifs used for coordination polymerization and interweavement This review is purposely directed to analyze the infinite disulfonate architectures with respect to their coordination entanglement and to reveal the role of, and the mutual interrelation, between variable structure controlling factors. In particular, the preferred structural motifs, used for formation and multidimensional extension of the crystal chemical units are addressed. For this reason the metal organic frameworks (MOF) are compared and systemized using a modified topological approach. Originally the principles for delineation of MOF were developed by Batten and Robson [6] and successfully used for a topological classification of variable interpenetrating nets [7]. However, for comparison reasons we have adopted a somewhat different approach which allows for specifying the individual coordination units and the motifs linking them into extended coordination framework [9].

2. General properties of sulfonic acids

Sulfonic acids are a class of compounds in which an R-group is attached to the sulfonic group. Usually they appear in zwitterionic forms, whenever there is a lone pair in the auxiliary R-group. Unlike the carbon atom, the central atoms of the sulfonic and phosphonic groups are able to accommodate more than eight electrons in the outer electron shell, which accounts for a greater bonding flexibility in these groups compared to the carboxylic group. However, the proton of the sulfonic group is more easily dissociable than the proton of the carboxylic group or the first proton of the phosphonic group and in this respect the sulfonic acids are stronger then their phosphonic and carboxylic analogues. On the other side, the disulfonic acids with a general formula SO_3H–R–SO_3H are bifunctional compounds, analogous to the diphosphonic and dicarboxylic acids. They fully deprotonate at very low pK_a, which causes serious problem with their stability. Usually, they are commercially available as sodium salts. Modification of the R spacer between the two sulfonic groups can lead to broad structural differentiations.

3. Hydrogen bond and coordination abilities of the sulfonate group

The sulfonic group very readily releases its proton in order to transform into a highly symmetric sulfonate group possessing a three-fold symmetry axis. Additionally, three symmetry planes (C_{3v}) should be taken into account considering the six electron pairs on the sulfonate oxygen atoms (Scheme 1). Therefore, the supramolecular chemistry of sulfonic acids is extremely exciting with respect to the ability of the sulfonate group to accept up to six hydrogen bonds along these lone pairs. The equal number of hydrogen bond donors and acceptors, located on two separated sites with matched geometry and stereoavailability, allows for a formation of persistent, six-member guanidinium sulfonate module. The (pseudohexagonal) module GS, resembling a rosette, is predisposed for further hydrogen bond recognition in order to form periodically extended, two-dimensional networks GS2 (see Scheme 2). All three hydrogen bonded motifs R2,2(8), used for generation of the network, represent

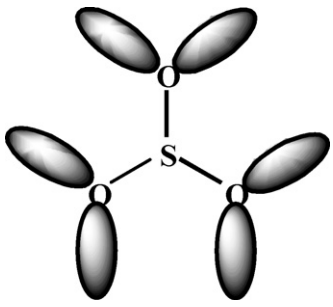

Scheme 1.

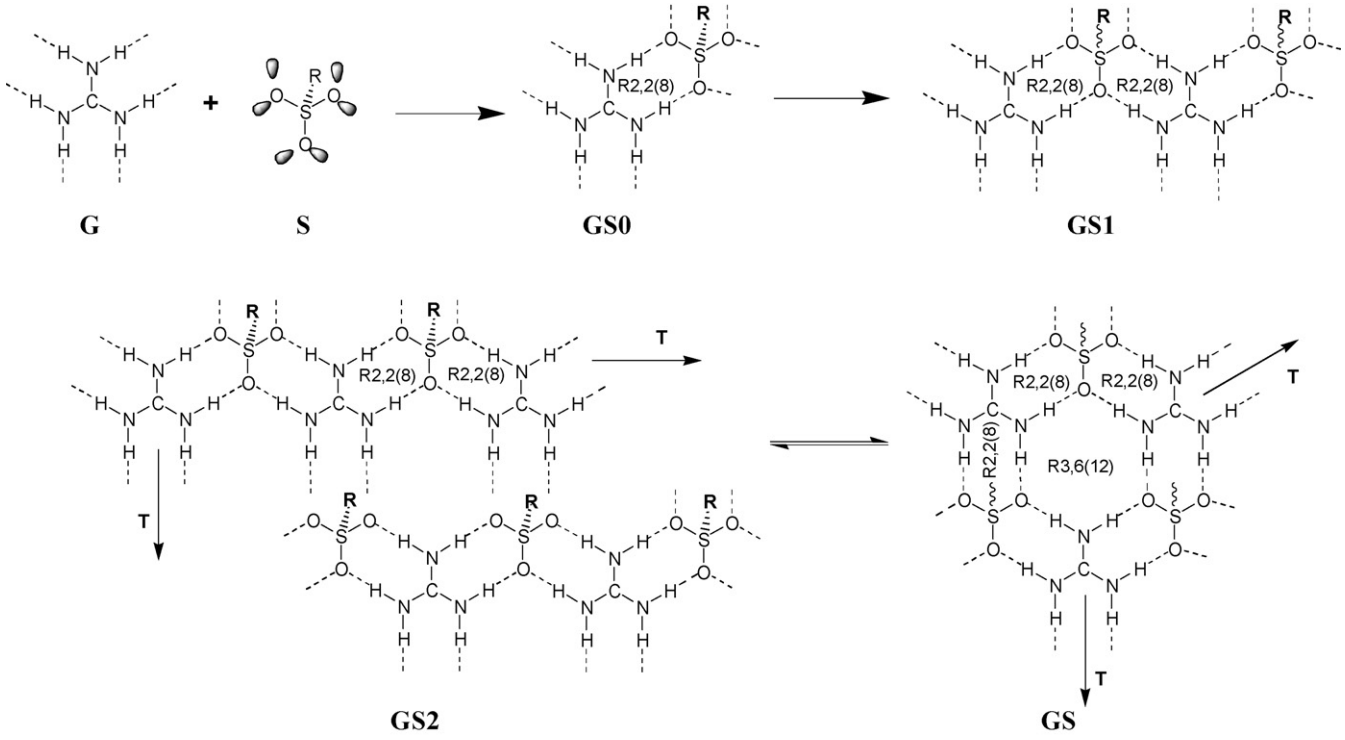

Scheme 2.

the same supramolecular synthon GS0. Guanidinium sulfonate compounds are a beautiful demonstration of saturated hydrogen bonded networks, issued by design. The guanidinium monosulfonates display variable mono- and bilayer structures [10–16], whereas the guandinium disulfonates merely form clathrate compounds with form and size controllable filaments depending upon the length and geometry of the R-spacer between the two sulfonate groups [19–25].

On the other hand, the same lone pairs (used as hydrogen bond acceptors in guanidinium sulfonate systems) can potentially donate up to six coordination bonds toward appropriate metal ions in order to form a number of sulfonato compounds. For example, the silver(I) complexes with methane- , ethane- and butanedisulfonic acids [70,71] demonstrate a "saturated coordination network". The sulfonate groups adopt variable coordination modes: $\eta^6\mu_6$, $\eta^5\mu_5$, and $\eta^4\mu_4$. Remarkably, the Ag ethane- and butanedisulfonate compounds display pillared structures, very similar to those observed in guanidinium disulfonates and the 2D coordination networks resemble the 2D hydrogen bonded networks presented in Scheme 2. Hydrogen bonded guanidinium sulfonates and disulfonates have been systematically studied by Ward [10–16,19–25]. The coordination chemistry of the sulfonate group and the structural properties of metal arenesulfonates have been explored by Côté and Shimazu [17], Cai [26] and many others.

4. Classification of sulfonic compounds

A survey, made in the Crystallographic Structural Database Cambridge (CSD v. 5.27) [18], reveals 5884 structures of various sulfonic compounds, 174 of which refer to pure acids and their derivatives. The rest, 5710 structures, belong merely to metal ion coordination complexes (1375 hits) and/or different ionic compounds (4056 hits)).

The present study is limited to 248 different disulfonate/disulfonato compounds. Although 60 of them display disordered structures, they are also included in the study, since the structural disorder, especially in the clathrate compounds, is implicated by the solvent molecules. Only three structures of pure disulfonic acids are found in the CSD and they present zwitterionic forms.

One hundred and fourteen structures (out of 248) belong to hydrogen bonded ionic complexes. Most of them (81 hits) present variable guanidinium disulfonates. The clathrate character of these systems has been extensively studied by the Minnesota group and presented in a series of papers [19–25]. The form and the size of the filaments therein are controllable and depend upon the length and geometry of the R-spacer between the sulfonate groups, which allows variable solvent molecules to be entrapped within. Thirty-five of these structures display disorder. The rest of the hydrogen bonded disulfonate compounds are divided as follows: ammonium/diammonium (eight hits), pyridinium/dipyridinium (six hits) and oxonium (three hits) disulfonates, cocrystals with protonated aminoacids (nine hits) or with nucleic bases (two hits), one crown ether, three cycloalkane disulfonates and 1 tetrathiafulvalene structures.

In accordance with the main object of the study, we concentrate, later, on the extended metal-organic frameworks (MOF) of the disulfonato coordination complexes. This class of compounds is represented by 134 structures and can be divided into four formal subclasses: group 1 metal ion complexes (29 structures); group 2 metal ion complexes (19 structures); transi-

tion metal ion complexes (71 structures) and f-block metal ion complexes (15 structures).

The alkaline metal ion complexes are not addressed in this paper since their structural chemistry and properties have been broadly discussed in a recent review by Cai [26]. The f-electron metal ion complexes are also excluded from the discussion. Hereafter, we focus on the group 2 (19 hits) and the transition metal ion (71 hits) coordination complexes. In particular we analyze the extended metal-organic and supramolecular networks therein. These compounds can be further divided into two subgroups: (a) disulfonate salts with no direct binding between the sulfonate moiety and the complex metal ion (41 hits); and (b) disulfonato coordination complexes (49 hits). Variable solvent molecules (predominantly (di)amines and/or water (19 hits)), serving as metal ligands, penetrate the first coordination sphere of the ion in the first subgroup (see Table 1), and efficiently prevent the disposal of the sulfonate oxygen atoms lone pairs.

5. Methodology

The structural analysis, performed for 90 coordination compounds of interest, reveals a variety of unit and polymer linking motifs. The structures range from isolated mononuclear, dinuclear and multinuclear coordination units (0D), to coordination chains (1D coordination frameworks) and coordination layers (2D frameworks) up to three-dimensional (3D) coordination frameworks. The plethora of structural motifs makes the characterization and comparison of the infinite architecture troublesome unless some comfortable notation for their description is used. A characteristic of the high-dimensional frameworks is that they are entangled and the individual units cannot be separated without breaking coordination bonds. In a former paper the description *Rm,d*(*n*) was adopted for identification of the ring motifs [9]. However, for the purposes of the present work one needs to introduce additional graph notations suitable for description of all observed coordination motifs. The following graph-sets are proposed: *Dm,d*(*n*) for the dinuclear coordination units with one ligand shared between the metal centers and *Cm,d*(*n*) for the repeating motifs in polymeric coordination chains. Again, *m* means the number of metal centers in the motif, *d* the number of atoms donating electron pair to the metal center and *n* is the number of coordination and covalent bonds counted along the shortest path. This shorthand is similar to that used for identification of hydrogen bonded motifs [27]. The graph-sets are informative about the size and the shape of the coordination units, as well as about the linking motifs and the distances between the metal centers in the extended coordination arrays. For example, graph R1,2(*n*) signifies the presence of a chelate ring and the denominator *n* apprises its size, while R2,4(*n*) informs that two metal ions are sharing ligand(s) in order to form a ring. On the other hand the graph-sets are advantageous in disentanglement and description of complicated coordination framework since they are informative about the phenomenon of catenation and the degree of catenation (DOC) as well as about the size of the meshes and cavities generated in the coordination framework. Each point (atom) in the closed circuit has two connection bonds with two neighbors. So, the numbers of donating atoms in the ring is equal to twice the number of the metal centers included in it. However, if the coordination species is entangled or catenated and one or more donating atoms in the circle are shared, the number *d* is correspondingly lower. *Rm,d*(*n*) and *Cm,d*(*n*) (instead *D*) are used for describing the periodically repeated motifs in the extended coordination arrays.

Hereafter we classify the disulfonate compounds with respect to their coordination species and delineate the high-dimensional frameworks.

6. Solvated metal ion disulfonates

Almost all solvated metal ion sulfonates (Table 1) display isolated monomeric coordination units (**1**–**34**). It is common for them that the metal units and the sulfonate portion are organized in separate cation–anion regions, which are further arranged in 3D via multiple hydrogen bonds established between the metal ligand sites (usually diamines and/or water molecules) and the sulfonate groups. Four compounds (**35**–**38**) present isolated dimers, one forms an isolated heteropolynuclear unit (**40**). In compound **41**, the neighboring inversion related ions $[Hg_2(H_2O)]^{2+}$ are sharing two $\eta^2\mu_2$ aqua ligands in order to form 1D polycationic chains via R2,2(4) motif. The multinuclear Co^{2+} compound **39** is very unusual and deserves some attention. The isolated coordination unit contains seven cobalt ions, 12 hydroxyl and two aqua ligands. The hydroxyl groups adopt the $\eta^3\mu_3$ mode, whereas the water molecules serve as $\eta^2\mu_2$ ligands. There are four crystallographically distinguished metal centers, three of which (Co1, Co2 and Co3) are octahedral. Co2 and Co3 form two independent coordination dimers Co2–Co2 and Co3–Co3, using two centrosymmetric R2,2(4) ring motifs. Another R2,2(4) motif, formed between Co2 and Co3 interlinks the dimers and extends them into coordination ribbons along the *a*-direction. Co1 interweaves the ribbons via two Co1–Co2 and Co1–Co3 R2,2(4) motifs in order to generate a buckled hexagon framework. Big six-center R6,6(12) rings are encircled between Co1, Co2 and Co3. Two inversion related Co4 ions protrude these hexagons. Co4 is four-coordinated and shares hydroxyl oxygen sites (Co4-O 1,95 Å) with Co1, Co2 and Co3. The fourth coordination bond Co4-Ow, formed with the aqua ligand, is significantly longer (2.1 Å). The angle relationship between the coordination bonds show that Co4 ion is forced to adopt a geometry close to trigonal pyramid in order to meet the symmetry requirements of the 2D framework. Variable ring motifs are generated in the two-dimensional entanglement of the Co cluster: R3,3(6) between each three different metal centers and R4,4(8)) between two pairs of inversion related Co4 and Co2 or Co4 and Co3 centers. The final outcome of the metal ion organization are thick coordination monolayers with Co1, Co2 and Co3 arranged in the interior and Co4 in the exterior (Fig. 1). The 1,2-etds anions are arranged between the coordination monolayers and serve to link them. The hydrogen atoms of the hydroxyl and aqua ligands protrude the interlayer regions and donate multiple hydrogen bonds toward the sulfonate oxygen atoms furnishing the supramolecular network.

Table 1
Coordination units and three-dimensional networks in disulfonate compounds with no direct binding between the sulfonate groups and the complex metal ion

Compound name	Ref. code	Space group	Coordination unit	Linking motifs	3D network	Reference
Isolated monomeric coordination units						
1. bis((Triethylenetetraamine)-(1,10-phenanthroline)-cobalt(iii)) tris(naphthalene-1,5-disulfonate) tetrakis(1,10-phenanthroline) clathrate hexadecahydrate	ASETAT	*C*2/*c*	Co(III)–octahedral		3D hydrogen bonded network	[28]
2. bis(bis(Ethylenediamine)-(1,10-phenanthroline)-cobalt(iii)) tris(naphthalene-1,5-disulfonate) tetradecahydrate	ASETEX	$P\bar{1}$	Co(III)–octahedral		3D hydrogen bonded network	[28]
3. Aqua-bis(2,2′-bipyridyl)-copper(ii) disulfonato-trisulfane	BPACUS	$P2_1/c$	Cu(II)–deformed square pyramid		1D hydrogen bonded network, 2D stacking interactions 3D electrostatic interactions	[29]
4. bis(bis(2,2′-Bipyridyl)-chloro-copper(ii)) disulfonato-trisulfane hexahydrate	BPCCUS	$C\bar{1}$	Cu(II)–deformed square pyramid			[29]
5. bis(Pyridinium) 1,5-naphthalenedisulfonate diaqua-tetrachloro-tin(iv)	FETHOC[a]	*C*2/*c*	Sn(IV)–octahedral		3D hydrogen bonded network; organic–inorganic regions along *a;* OFF and EF interactions inside the organic region	[30]
6. Hexa-aqua-zinc(ii) naphthalene-1,5-disulfonate	FOGWUU	$P2_1/c$	Zn(II)–octahedral		3D hydrogen bonded network; organic–inorganic regions along *a*, EF interactions inside the organic region	[31]
7. Diaqua-bis(1,10-phenanthroline)-zinc(ii) 4,5-dihydroxy-1,3-benzenedisulfonate trihydrate	FIMBEL	$P\bar{1}$	Zn(II)–octahedral phen: $\eta^2\mu_1$–ligand two R1,2(5) coord. rings		3D hydrogen bonded network	[32]
8. s-fac-bis((Diethylenetriamine)-(3-methyl-1,5-diamino-3-azapentane)-cobalt(iii)) disulfonate monohydrate	JULTER	$P2_1$	Co(III)–octahedral two: $\eta^3\mu_1$–ligands four R1,2(5) coord. rings		3D hydrogen bonded network	[33]
9. Hexa-aqua-cobalt(ii) 1,5-naphthalenedisulfonate	IRONIUM	$P2_1/c$	Co(II)–octahedral		3D hydrogen bonded network	[34]
10. Hexa-ammine-cobalt 1,4-bis(2-sulfonatoethyl)piperazine chloride hexahydrate	WABXUT[a]	*P*1	Co(II)–octahedral		3D hydrogen bonded network; Hydrophilic hydrophobic regions.	[35]
11. Hexa-aqua-nickel(ii) naphthalene-1,5-disulfonate	LUMVAQ	$P2_1/c$	Ni(II)–octahedral		3D hydrogen bonded network	[36]
12. *trans*-Diaqua-bis(ethylenediamine-*N*,*N*′)-nickel(ii) naphthalene-1,5-disulfonate dihydrate	LUMVEU	*C*2/*c*	Ni(II)–octahedral		3D hydrogen bonded network	[36]
13. Diaqua-(tris(2-aminoethyl)amine-*N*,*N*′,*N*″)-nickel(ii) naphthalene-1,5-disulfonate monohydrate	LUMVIY	$P\bar{1}$	Ni(II)–octahedral		3D hydrogen bonded network	[36]
14. bis(bis(2-Aminoethyl)amine)-nickel(ii) naphthalene-1,5-disulfonate dihydrate	LUMVOE	$P2_1/c$	Ni(II)–octahedral		3D hydrogen bonded network	[36]
15. bis(L-Arginine-*N*,*O*)-copper(ii) 1,3-benzenedisulfonate	MARTOO	*C*2	Cu(II)–square planar		(001) hydrogen bonded monolayers; 3D hydrogen bonded network	[37]
16. bis(bis(Nicotinamide)-silver(i)) 4,4′-biphenyldisulfonate dihydrate	MOFLIC	$P\bar{1}$	Ag(I)-linear		3D hydrogen bonded network	[38]
17. bis(bis(Nicotinic acid)-silver(i)) naphthalene-1,5-disulfonate dihydrate	MPFLOU	*C*2/*c*	Ag(I)-linear		Separated cation and anion regions, hydrogen bonded in 3D	[38]
18. (μ_2-2,5-bis(2-Pyridyl)pyrazinato)-bis(tetra-aqua-nickel(ii)) disulfonate dihydrate	NEVGOK	$P2_1/n$	Ni(II)-octahedral		(110) hydrogen bonded monolayers; 3D hydrogen bonded network	[39]
19. Hexa-aqua-nickel(ii) 3-ammonionaphthalene-1,5-disulfonate tetrahydrate	NIHSAY	$P\bar{1}$	Ni(II)-octahedral		Separated cation and anion regions, hydrogen bonded in 3D	[40]
20. Diaquabis(ethylenediamine)copper(ii) bis(tris(ethylenediamine)nickel(ii)) tris(naphthalene-2,6-disulfonate) tetrahydrate	TIJGAU	$P\bar{1}$	Cu(II)–octahedral Ni(II)-octahedral		3D hydrogen bonded network	[41]
21. tris(Ethylenediamine-*N*,*N*′)-nickel(ii) perfluoropropane-1,3-disulfonate	UBEHOY	$P2_1/c$	Ni(II)-octahedral		1D hydrogen bonded network	[42]
22. (1,4,8,11-Tetra-azacyclotetradecane-*N*,*N*′,*N*″,*N*‴)-diaqua-cobalt(ii) 1,5-naphthalenedisulfonate dihydrate	UKETAF	$P\bar{1}$	Co(II)-octahedral		Separated cation/anion regions, hydrogen bonded in 3D	[43]
23. bis(Hexa-ammine-cobalt) tris(naphthalene-2,6-disulfonate) dioxane solvate hydrate	WABYAA	*C*2/*c*	Co(II)-octahedral		Separated cation/anion regions, hydrogen bonded in 3D	[35]

Table 1 (*Continued*)

Compound name	Ref. code	Space group	Coordination unit	Linking motifs	3D network	Reference
24. Tetraaqua-bis(nicotinamide)-copper(ii) 4,4′-biphenyldisulfonate	XABNUC	$P\bar{1}$	Cu(II)-octahedral		3D hydrogen bonded network	[44]
25. Tetraaqua-bis(nicotinamide)-copper(ii) naphthalene-2,6-disulfonate dihydrate	XABPAS	$P\bar{1}$	Cu(II)-octahedral		3D hydrogen bonded network	[44]
26. bis(Ethylenediamine)-copper(ii) naphthalene-1,5-disulfonate dihydrate	XEPGII	$P4_12_12_1$	Cu(II)–square planar		3D hydrogen bonded network	[45]
27. Diaqua-bis(1,2-diaminopropane)-copper(ii) naphthalene-1,5-disulfonate	XEPHEF	$P2_1/n$	Cu(II)-octahedral		3D hydrogen bonded network	[45]
28. Diaqua-bis(*N*,*N*′-dimethylethylenediamine)-copper(ii) naphthalene-1,5-disulfonate monohydrate	XEPHIJ	$P\bar{1}$	Cu(II)-octahedral		3D hydrogen bonded network	[45]
29. tris(Ethylenediamine-*N*,*N*′)-nickel(ii) naphthalene-2,6-disulfonate monohydrate	YAFSOO	$P2_1/n$	Ni(II)-octahedral		3D hydrogen bonded network	[46]
30. tris(Ethylenediamine-*N*,*N*′)-nickel(ii) difluoromethanedisulfonate	UBEHIS	*Pbcn*	Ni(II)–octahedral en: $\eta^2\mu_1$–ligands, three R1,2(5) coord. rings		3D hydrogen bonded network with hydrophobic channels along *c*-axis	[42]
31. Hexa-aqua-magnesium(ii) 1,5-naphthalenedisulfonate	RAKYOR	$P2_1/c$	Mg(II)–octahedral		Inorganic/organic regions along *b;* 3D hydrogen bonded network	[47]
32. Hexaaqua-magnesium 4,5-dihydroxybenzene-1,3-disulfonate trihydrate	OMARID	$P\bar{1}$	Mg(II)–octahedral	$Mg^{2+}(H_2O)_6$–h.b. dimers	(010) layers via aqua-sulfonate hydrogen bonds; 3D hydrogen bonded network	[48]
33. Hexa-aqua-magnesium 7-hydroxy-8-(phenylazo)-1,3-naphthalenedisulfonic acid dihydrate	WIKXAP	$P\bar{1}$	Mg(II)–octahedral		3D hydrogen bonded network	[49]
34. Hepta-aqua-calcium 7-hydroxy-8-(phenylazo)-1,3-naphthalenedisulfonic acid dihydrate	WIKXET[a]	$P2_1/n$	Ca(II)–monocapped octahedral		3D hydrogen bonded network	[49]
Isolated multinuclear coordination units						
35. bis(μ_2-2,6-bis(1-Methylbenzimidazol-2-yl)pyridine-di-copper(i)) naphthalene-1,5-disulfonate	JARDIP	*Cc*	Cu(I) intermediate between square planar and tetrahedral	Cu-Cu dimers R2,2(4)	(100) monolayers via stacking interactions; interlayer hydrophobic interactions	[50]
36. bis(μ_2-Chloro)-bis(2-(*N*,*N*-bis(2-aminoethyl)amino) ethylammonium-*N*,*N*′,*N*″)-di-copper(ii) bis(naphthalene-1,5-disulfonate) pentahydrate	YOJNEQ	$P\bar{1}$	Cu(II) deformed trigonal bipyramid two $\eta^3\mu_1$–ligands	Cu-Cu dimers R2,2(4)	3D hydrogen bonded network; alternating anionic–cationic regions along *b*-axis	[51]
37. (μ_2-2,5-bis(2-Pyridyl)pyrazinato)-bis(tetra-aqua-nickel(ii)) disulfonate dihydrate	NEVGOK	$P2_1/n$	$\eta^4\mu_2$ ligand, two R1,2(5) chelate rings	D2,2(6)	(1 0 $\bar{1}$) hydrogen bonded monolayer via coordination water–sulfonate interactions; 3D hydrogen bonded network via crystalline water–sulfonate interactions	[52]
38. *cis*-(μ_2-(*N*,*N*′-bis(2-Aminoethyl)-1,2-ethanediamine)-bis(*N*,*N*′-bis(2-aminoethyl)-1,2-ethanediamine))-di-nickel(ii) tetrakis(4,4′-biphenyldisulfonate) tetrahydrate	SUWZAL	*C*2	Ni(II)–octahedral; two $\eta^4\mu_1$ and one bridging $\eta^4\mu_2$ *N*,*N*′-dien ligands; three chelate rings R1,2(5)	D2,2(5)	3D hydrogen bonded network	[53]
39. catena-(dodecakis(μ_3-Hydroxo)-diaqua-hepta-cobalt(ii) ethylene-1,2-disulfonate) $[Co_7(H_2O)_2(HO)_{12}]$(1,2-etds)	INRIG	$P\bar{1}$	Co1, Co2, Co3 octahedral; Co4 trigonal pyramid; OH: $\eta^3\mu_3$ ligand; H_2O: $\eta^2\mu_2$ ligand	R2,2(4) (1D) R3,3(6) (2D) R4,4(8) (2D) R6,6(12) (2D)	Multiple hydrogen bond interactions: Hydroxyl–water, hydroxyl– sulfonate, water–water hydrogen bonds O-H···O	[54]
Isolated (hetero)polinucler multimers						
40. catena-(hexakis(μ_2-Cyano)-hexa-cyano-octakis(1,1-dimethylethylenediamine)-diaqua-di-iron-tetra-nickel biphenyl-4,4′-disulfonate hexahydrate)	WUCNIR	$P2_1/c$	Fe–octahedral Ni-octahedral	1D coord framework	3D hydrogen bonded network	[55]
1D mononuclear coordination polymers						
41. catena-(bis((μ_2-Aqua)-((μ_2-1,5-naphthalenedisulfonato-*O*,*O*′)-bis(aqua-mercury(i)))	FETHUI	$P2_1/n$	Hg deformed tetrahedral; two $\eta^2\mu_2$ water ligands	Hg-Hg dimers R2,2(4)	1D coord. array via Hg-Hg coord. bridge; 3D hydrogen bonded network via coord. water–sulfonate interactions	[56]

[a] Disordered structures.

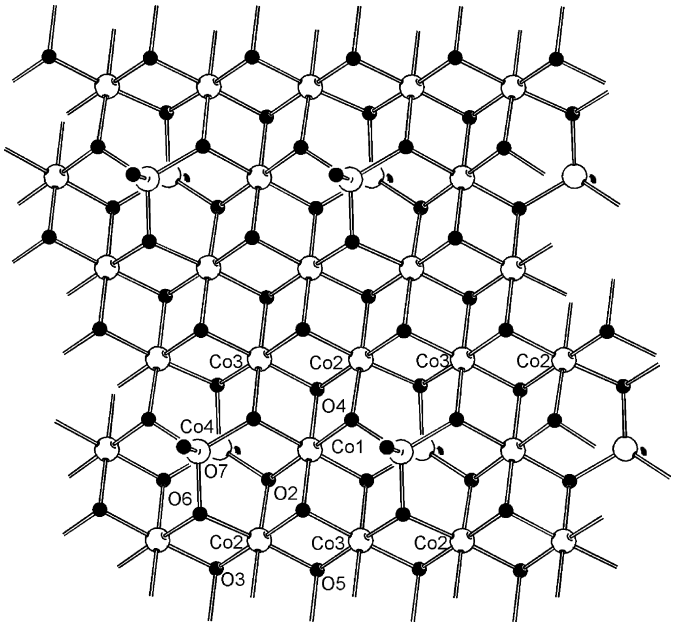

Fig. 1. The coordination monolayer $[Co_7(H_2O)_2(OH)_{12}]$ in compound **39** (Ref. [54]). The hydrogen atoms of the ligands are omitted.

7. Delineation of the coordination frameworks of transition metal ion complexes

Complete structural information concerning the coordination units, linking motifs and the crystal networks observed in this group of compounds is presented in Table 2. While the formerly studied bisphosphonate systems demonstrate a tendency for bidentate coordination [9], a monodentate coordination is preferred in the disulfonate systems. Therefore, chain motifs *Cm*,*d*(*n*) (not *Rm*,*d*(*n*) ring motifs) are predominantly employed for the extension of the individual coordination units. Most of the compounds studied display 1D coordination species and only a few of them form 2D and 3D coordination frameworks.

7.1. Isolated coordination units

Compounds **42**–**50** reveal structures with isolated coordination units. Their metal ions are octahedral (except for one of the copper(II) ions in **50**). Compounds **42**–**44** display mononuclear coordination units, and compounds **45**–**50** are multinuclear (Fig. 2). The disulfonate ligands in all but one, complexes are monodentate. The nickel compound **42** deserves some attention, since this is one of the rare examples of bidentate binding of the metal ion by the disulfonate ligand. The *ortho*-position of the sulfonic groups in 1,2-bds allows for metal chelation with a seven-member ring motif R1,2(7). (Fig. 2a) The coordination units are organized in (*ab*) bilayers via off-set face-to-face (OFF) and edge-to-face (EF) interactions between the aromatic rings of the ligands. The solvent molecules are entrapped in hydrophobic pockets generated between four inversion related units (of two neighboring layers). However, the absence of hydrogen bond donors and therefore of stabilizing interactions in the system leads to dynamic disorder of the solvent, since the dimethylformamide oxygen tries to stay as far as possible from the sulfonate oxygen atoms.

Compounds **45** and **46** consist of dinuclear coordination units with a D2,2(9) motif. Compounds **47**–**49** are coordination dimers with R2,4(8) motif formed between the two metal ions (Fig. 2b). The building unit in the tetranuclear compound **50** can be considered to be a centrosymmetric coordination dimer consisting of two dinuclear Cu1–Cu2 subunits (Fig. 3a). The two symmetry independent ions display different coordination geometries, square pyramidal for Cu1 and distorted octahedral for Cu2. The nature and the geometry of the 2,6-ipds ligand allow for a tridentate equatorial binding to each metal center (via two pairs of R1,2(5) and R1,2(6) chelate rings) in order to form the subunit. Additionally one of the sulfonate groups, adopting a $\eta^2\mu_2$ mode, binds Cu2 of the inversion related subunit. The hydroxy group is coordinated in $\eta^3\mu_3$ fashion and serves as an equatorial ligand to each ion of the subunit and additionally acts as an axial ligand to Cu1 of the inversion related subunit. So, the dinuclear Cu1–Cu2 subunits are interplayed at four points via the $\eta^3\mu_3$ hydroxyl ligand and the $\eta^2\mu_2$ sulfonate site of the 2,6-ipds ligand. The resultant centrosymmetric tetranuclear coordination unit displays the shape of an incomplete double cube with metal centers interlinked by five R2,2(4) catenating motifs, four of which are established between symmetry distinct Cu1–Cu2 ions and the fifth one is between Cu1–Cu1 ions. Two rings R3,3(6) are closed between Cu1–Cu1–Cu2 centers, whereas all four Cu centers of the unit encircle two R4,4(8) motifs. The tetranuclear units are organized in monolayers. The crystalline water molecules are arranged between the monolayers and hydrogen bond them into a 3D supramolecular network (Fig. 3b).

Generally, the hydrogen bonds govern the organization of the isolated coordination units in compounds **42**–**50**, although stereo and packing effects dictated by ligands are also important.

7.2. One-dimensional coordination networks

Compounds **51**–**65** display one-dimensional coordination arrays. The end positions of the sulfonate groups in the R-spacer facilitates the polymeric extension of the metal ions unless some severe impediments from the auxiliary ligands are imposed. Therefore, we present the structure of these compounds in view of the metal ion coordination geometry on the one hand and the ligands' binding modes on the other. In particular, the size and the topological symmetry of the disulfonate ligand bridging the metal centers in coordination chains, is discussed with respect to the 3D unit arrangement and packing consequences. The role of the auxiliary ligands is also considered.

Compound **51** is very specific. The octahedral copper ion is equatorially coordinated by four N-atoms of the 5-cyclam ligand in order to form two R1,2(6) chelate rings with chair conformation and two R1,2(5) chelate rings with half-chair conformation. The meds ligand bridges with $\eta^1\mu_1$ modes the neighboring, translation related Cu-cyclam units in order to extend them into one-dimensional C1,2(5) arrays. The four hydrogen atoms, located on the coordinated N-atoms obtain axial positions versus the cyclam plane and donate four intrachain hydrogen bonds

Table 2
Coordination units, linking motifs and three-dimensional networks in transition metal ion complexes

Compound name/formula	Ref. code	Space group	Configuration of the coord. unit(s)/ligand binding mode(s)	Linking motif(s)/1D array(s) formed by disulfonate ligands	3D network	Reference
0D frameworks (isolated coordination units)						
42. bis(2,2-Bipyridine)-(benzene-1,2-disulfonato-*O*,*O*′)-nickel(ii) dimethylformamide solvate [Ni(1,2-bds)(2,2-bpy)$_2$].(dmf)	BAMPOU[a]	$P\bar{1}$	Ni(II)–octahedral: 3 chelate rings: 1,2-bds: $\eta^2\mu_1$ ligand, chelate R1,2(7); 2,2-bpy: $\eta^2\mu_1$ ligand, chelate R1,2(5)		Ni-units are organized in (ab) bilayers; solvate molecule between the layers	[57]
43. Aqua-bis(2,2′-bipyridine-*N*,*N*′)-(4,4′-diphenyl ether disulfonato-*O*)-cadmium(ii) tetrahydrate [Cd(peds)(2,2-bpy)$_2$(H$_2$O)]·4(H$_2$O)	UGOWES	$P2_1/n$	Cd(II)–octahedral: peds: $\eta^1\mu_1$ ligand; 2,2-bipy: $\eta^2\mu_1$ ligand, chelate R1,2(5)		Hydrogen bonded 3D network	[58]
44. Tetraaqua-bis(nicotinamide)-copper(ii) diaqua-bis(naphthalene-1,5-disulfonate)-bis(nicotinamide)-copper(ii) octahydrate [Cu(1,5-nds)$_2$(inia)$_2$(H$_2$O)$_2$] [Cu(inia)$_2$(H$_2$O)$_4$]·8H$_2$O	XABPEW	$C2/c$	Cu1, Cu2–octahedral, $\eta^1\mu_1$ ligands		Hydrogen bonded 3D network	[43]
Isolated multinuclear coordination units						
45. (μ_2-1,5-Naphthalenedisulfonato)-bis(di-*n*-butyl-triaqua-tin) 1,5-naphthalenedisulfonate methanol solvate dihydrate [Sn$_2$(but)$_4$(H$_2$O)$_6$(1,5-nds)](1,5-nds).(met)·2H$_2$O	ELECON	$P\bar{1}$	Sn(II)–octahedral; 1,5-nds: $\eta^2\mu_2$ ligand; $\eta^1\mu_1$ ligands	D2,2(9)	Hydrogen bonded 3D network	[59]
46. (μ_2-1,5-Naphthalenedisulfonato-*O*,*O*′)-diaqua-tetrakis(2,2′-bipyridine-*N*,*N*′)-di-cadmium(ii) (1,5-naphthalenedisulfonate) tetrahydrate [Cd$_2$(2,2-bpy)$_4$(H$_2$O)$_2$(1,5-nds)](1,5-nds)·4H$_2$O	UGOWIW[a]	$P\bar{1}$	Cd(II)–octahedral 1,5-nds: $\eta^2\mu_2$ ligand; 2,2-bpy: $\eta^2\mu_1$ ligand, chelate R1,2(5)	D2,2(9)	Hydrogen bonded 3D network	[58]
47. bis(μ_2-1,5-Naphthalenedisulfonato-*O*,*O*′)-bis(1,4,8,11-tetra-azacyclotetradecane)-di-cadmium(ii) [Cd(4-cyclam)(1,5-nds)]$_2$	UGOWOC	$P2_1/n$	Cd(II)–octahedral; 4 chelate rings; 1,5-nds: $\eta^2\mu_2$ ligand; 4-cyclam: $\eta^4\mu_1$ ligand	Cd–Cd dimer via R2,4(8) coord. motif	Hydrogen bonded 3D network	[58]
48. (μ_2-1^5,11^5-Di-t-butyl-3,6,9,13,16,19-hexamethyl-3,6,9,13,16,19-hexa-aza-1,11(1,3)dibenzenacyclo-icosaphane-1^2,11^2-disulfonato-*O*,*O*′)-(μ_2-3-chlorobenzoato)-di-nickel(ii) tetraphenylborate ethanol solvate dihydrate	FAYXOT	$C2/c$	Ni(II)–octahedral; chlorobenzoate: $\eta^2\mu_2$; ligand; macrocycle with four coord. sites: two $\eta^3\mu_1$ ligand sites (*N*,*N*′,*N*″) and $\eta^2\mu_2$ ligand sites (*O*,*O*′)	Ni–Ni dimer via two different R2,4(8) coord. motifs	3D hydrogen bonded network with hydrophobic channels along *c*-axis	[60]
49. (μ_2-1^5,11^5-Di-t-butyl-3,6,9,13,16,19-hexamethyl-3,6,9,13,16,19-hexa-aza-1,11(1,3)dibenzenacyclo-icosaphane-1^2,11^2-disulfonato)-(μ_2-chloro)-di-nickel(ii) tetraphenylborate acetonitrile ethanol solvate	FAYXUZ	$P2_1/c$	Ni(II)–octahedral; macrocycle with four coord. sites: two $\eta^3\mu_1$ ligand sites (*N*,*N*′,*N*″) and $\eta^2\mu_2$ ligand sites (*O*,*O*′)	Ni–Ni dimer via two different coord. motifs: R2,4(8) and R2,3(6)	3D hydrogen bonded network	[60]
50. bis(μ_2-4-Chloro-2,6-bis((((sulfonato)methyl)imino)methyl)phenolato-*N*,*N*′,*O*,*O*′,*O*″)-bis(μ_3-hydroxo)-tetra-copper(ii) dimethylsulfoxide solvate dihydrate [{Cu$_2$(OH)(2,6-ipds)}(dms)]$_2$·H$_2$O	GADRAE[a]	*Pbca*	Cu1-square pyramidal, Cu2–octahedral; 2,6-ipds: $\eta^7\mu_3$ ligand; OH$^-$: $\eta^3\mu_3$ ligand; dms: $\eta^1\mu_1$ ligand	Cu1–Cu2 units interplayed at four points via three R2,2(4) motifs to form a tetranuclear coord. dimer; R3,3(6) between each three Cu centers; R4,4(8) between four Cu centers	Cu-tetranuclear coord. units are organized in (001) monolayers; crystalline water molecules link the monolayers into 3D hydrogen bonded network.	[61]
1D coordination frameworks						
51. (13-Methyl-6-(1-phenylethyl)-1,4,6,8,11-pentaazacyclotetradecane)-(disulfonato)-copper(ii) [Cu(5-cyclam)(meds)]	AXIPEC	$P3_1$	Cu–octahedral; two pairs of chelate rings: R1,2(5) and R1,2(6); meds: $\eta^2\mu_2$ ligand; 5-cyclam: $\eta^4\mu_1$ ligand;	Three 3-rotation related coord. chains C1,2(5) extended along [1 0 0], [0 1 0] and [1 1 0] directions.	Hydrogen bonds along the chains; hydrophobic interactions between the chains	[62]
52. catena((μ_2-Ethane-1,2-disulfonato)-tetra-aqua-copper(ii)) [Cu(H$_2$O)$_4$(1,2-etds)]$_n$	ETDESCU	$P\bar{1}$	Cu1 and Cu2–octahedral; 1,2-etds: $\eta^2\mu_2$ ligand	C1,2(7)–Cu1 chains [$\bar{1}$ 1 0] C1,2(7)–Cu2 chains [1 1 0]	Hydrogen bonded ($\bar{1}$ 1 1) monolayer; porous 3D network	[63]
53. catena-((μ_2-Butane-1,4-disulfonato-*O*,*O*′)-tetra-aqua-copper(ii)) [Cu(H$_2$O)$_4$(1,2-buds)]$_n$	BUDSCU	$P2_1/c$	Cu–octahedral; 1,4-buds: $\eta^2\mu_2$ ligand	C1,2(9)-chains along [1 0 0]	Hydrogen bonded (102) monolayers; hydrogen bonded 3D	[64]
54. catena-((μ_2-1,5-Naphthalenedisulfonato)-aqua-bis(triphenyl-tin) tetrahydrofuran solvate)	ELECUT	$P2_1/c$	Sn1, Sn2–trigonal bipyramid; 1,5-nds: $\eta^3\mu_3$ ligand	C1,2(9) helical chains along *b*	Hydrogen bonded (001) monolayers; hydrophobic interactions between them	[59]
55. catena-((μ_2-Naphthalene-1,5-disulfonato)-tetrapyridine-copper(ii)) [Cu(py)$_4$(1,5-nds)]	FOBVUO[b]	$P\bar{1}$	Cu–octahedral 1,5-nds: $\eta^2\mu_2$ ligand	C1,2(9) chains along [1 1 $\bar{1}$]	Hydrophobic interactions between the chains	[66]
56. catena-((μ_2-Naphthalene-1,5-disulfonato-*O*,*O*′)-(1,4,8,11-tetra-azacyclotetradecane-*N*,*N*′,*N*″,*N*‴)-nickel(ii) hydrate) [Ni(4-cyclam)(1,5-nds)]$_n$·*n*H$_2$O	UKESUY	$P2_1/c$	Ni–octahedral; 1,5-nds: $\eta^2\mu_2$ 4-cyclam: $\eta^4\mu_1$ ligand; chelate rings	C1,2(9) chains along [1 1 0] and [1 $\bar{1}$ 0] directions, N–H···O(S) along the chains	3D hydrogen bonded network via crystalline water molecules; channels along the *c*-axis	[43]
57. catena-[(μ_2-Naphthalene-1,5-disulfonato)-bis(*N*,*N*′-dimethylethylenediamine)-cadmium(ii)] [Cd(*N*,*N*′-meen)$_2$(1,5-nds)]$_n$	NELXIL	$P\bar{1}$	Cd–octahedral; 1,5-nds: $\eta^2\mu_2$ ligand; *N*,*N*′-meen: $\eta^2\mu_1$ ligand via R1,2(5)	C1,2(9) chains along [1 $\bar{1}$ 0]	(001) monolayers via N–H···O(S) hydrogen bonds; hydrophobic interactions between them	[65]
58. catena-[(μ_2-Naphthalene-2,6-disulfonato)-bis(*N*,*N*′-dimethylethylenediamine)-cadmium(ii)] [Cd)(*N*,*N*′-meen)$_2$(2,6-nds)]$_n$	NELXEH	$P2_1/c$	Cd–octahedral; 2,6-nds: $\eta^2\mu_2$ ligand; *N*,*N*′-meen: $\eta^2\mu_1$ ligand via R1,2(5)	C1,2(11) chains along [1 0 $\bar{1}$] N–H. . .O(S) along the chains	Hydrophobic interactions between the chains	[65]

59. catena-[(μ_2-Naphthalene-2,6-disulfonato)-bis(*N*-methylethylenediamine)-cadmium(ii) dihydrate] [Cd(*N*-meen)$_2$(2,6-nds)]$_n$·2*n*H$_2$O	NELXUX	$P2_1/n$	Cd–octahedral; 2,6-nds: $\eta^2\mu_2$ ligand; *N*-meen: $\eta^2\mu_1$ ligand via R1,2(5)	C1,2(11) chains along [1 1 0], [1 $\bar{1}$ 0] directions	(001) monolayers hydrogen bonded in 3D via crystal water molecules	[65]
60. catena-((μ_2-Naphthalene-2,6-disulfonato)-bis(*N*-methylethylenediamine)-copper(ii) dihydrate) [Cu(*N*-meen)$_2$(2,6-nds)]$_n$·2*n*H$_2$O	XEPGOO	$P2_1/n$	Cu–octahedral; 2,6-nds: $\eta^2\mu_2$ ligand; *N*-meen: $\eta^2\mu_1$ ligand via R1,2(5)	C1,2(11) chains along [1 1 0] and [1 $\bar{1}$ 0] directions	(001) monolayers hydrogen bonded in 3D via crystal water molecules	[44]
61. catena-((μ_2-2,6-Naphthalenedisulfonato-*O*,*O*′)-diaqua-bis(isonicotinamide-*N*)-cadmium(ii) tetrahydrate) [Cd(inia)$_2$(H$_2$O)$_2$(2,6-nds)]$_n$ 4*n*(H$_2$O)	UGOWUI	$P\bar{1}$	Cd1–octahedral; 2,6-nds: $\eta^2\mu_2$ ligand; inia and aqua: $\eta^1\mu_1$ ligands	C1,2(11) chains along [0 1 $\bar{1}$]; h. bonded (100) monolayers via aqua-sulfonate O(w)–H···O(S)	Intralayer aromatic interactions; interlayer amide–sulfonate N–H···O(S); water channels along [1 0 0] direction.	[58]
62. catena-((μ_2-4,4′-Biphenyldisulfonato)-bis(2,3-diaminopropane)-copper(ii)) [Cu(dapn)$_2$(bpds)]$_n$	XEPGUU[a]	$C2/c$	Cu–octahedral; bpds: $\eta^2\mu_2$ ligand; dapn: $\eta^2\mu_1$ ligand via R1,2(5)	C1,2(13) chains along [1 0 1]	3D hydrogen bonded network via amino–sulfonate interactions	[44]
63. catena-[(μ_2-4,4′-Biphenyldisulfonato)-bis(*N*,*N*′-dimethylethylenediamine)-cadmium(ii)] [Cd(*N*,*N*′-meen)$_2$(bpds)]$_n$	NELXOR	$P\bar{1}$	Cd–octahedral; bpds: $\eta^2\mu_2$ ligand; *N*,*N*′-meen: $\eta^2\mu_1$ ligand via R1,2(5)	C1,2(13) chains along [$\bar{1}$ 1 1]	(011) hydrogen bonded monolayers via N–H···O(S); interlayer hydrophobic interactions	[65]
64. catena-((μ_2-4,4′-Biphenyldisulfonato-*O*,*O*′)-diaqua-bis(isonicotinamide-N)-cadmium(ii) tetrahydrate) [Cd(inia)$_2$(H$_2$O)$_2$(bpds)]$_n$·4*n*H$_2$O	UGOXAP	$P\bar{1}$	Cd1–octahedral; bpds: $\eta^2\mu_2$ ligand; inia and aqua: $\eta^1\mu_1$ ligands	C1,2(13) chains along [0 $\bar{1}$ 1]; h. b. (0 $\bar{1}$ 1) monolayers via aqua-sulfonate O(w)–H···O(S)	Intralayer aromatic interactions; interlayer amide–sulfonate N–H···O(S); 3D h.b. network via crystal water	[58]
65. catena-((μ_3-4,4′-Diphenyl ether disulfonato-*O*,*O*′,*O*″)-(μ_2-4,4′-diphenyl ether disulfonato-*O*,*O*′)-triaqua-tetrakis(isonicotinamide-N)-di-cadmium(ii) dihydrate) [Cd$_2$(inia)$_4$(H$_2$O)$_3$(peds)$_2$]$_n$·2*n*H$_2$O	UGOXET	$P\bar{1}$	Cd1 and Cd2–octahedral; peds1: $\eta^2\mu_2$ ligand; peds2: $\eta^3\mu_3$ ligand; inia and aqua: $\eta^1\mu_1$ ligands	Cd1–Cd2 units via D2,2(14) coord. motif; ribbon extensions via two R2,2(8) linking motifs: Cd1–Cd1 and Cd2–Cd2; C3,4(28) periodical distance	Aqua–sulfonate h.b. interactions join the coord. ribbons into (0 1 $\bar{2}$) monolayer; Amide–sulfonate h.b. interactions cross-link the monolayers into 3D supramolecular network.	[58]
2D coordination frameworks						
66. catena((μ_3-Methanedisulfonato)-tri-aqua-cadmium) [Cd(H$_2$O)$_3$(meds)]$_n$	CAMSOB01	$P2_1/n$	Cd–pentagonal bipyramid; meds: $\eta^4\mu_3$ ligand; bidentate bonding to form chelate ring R1,2(6)	Two different linking motifs: C1,2(4) along [1 0 0], C1,2(4) along [1 0 1]; R3,6(14) windows	Coordination interplay of chelate units via C1,2(4) motifs to form (*ac*) layers; intra a. interlayer aqua–sulfonate h.b.	[67]
67. catena((μ_3-Methanedisulfonato)-tri-aqua-cadmium) [Cd$_2$(H$_2$O)$_6$(meds)$_2$]$_n$	CAMSOB	$P\bar{1}$	Cd1, Cd2–pentagonal bipyramids; two distinct $\eta^4\mu_3$ ligands forming two chelate coord. units R1,2(6)	Cd1 chains via C1,2(4), Cd2 chains via C1,2(4); two different R3,6(14)	Cd1, Cd2 chains interweaved via C1,2(4) to form (*ac*) coord. layer; intra a. interlayer aqua–sulfonate h.b	[68]
68. catena-(tetrakis(μ_4-1,5-Naphthalenedisulfonato)-octa-aqua-tetra-cadmium(ii)) [Cd$_4$(H$_2$O)$_8$(1,5-nds)$_4$]$_n$	UGOXIX	$P\bar{1}$	Cd–deformed octahedral; 1,5-nds: $\eta^4\mu_4$ ligands; aqua: $\eta^1\mu_1$ ligands	Cd1–Cd1, C2–Cd3 interplayed in 2D network via R2,4(8); C3,4(8) periodical distance	(1 1 $\bar{1}$) coord. monolayer: intralayer EF, interlayer aqua-sulfonate h. bonds; organic/inorganic regions	[58]
69. catena-((μ_9-*N*-Isopropylimino-bis(methylphosphonato))-(μ_7-*N*-isopropylimino-bis(methylphosphonato))-(μ_6-*N*-isopropylimino-bis(methylphosphonato))-(μ_2-3-sulfonatobenzoato)-diaqua-hepta-lead(ii) dihydrate)	EWUTAR[a]	$P\bar{1}$	Pb1 Pb2 Pb3 Pb4	Multiple R2,2(4) ring link the Pb centers into (010) coordination monolayers.	Interlayer hydrogen bonds join the monolayers into 3D supramolecular network.	[69]
3D coordination frameworks						
70. Silver(i) syn/anti-methane-disulfonate [Ag$_4$(meds)$_2$]$_n$	MEDSUL	$Pmc2_1$	Ag1-distorted octahedral, Ag2–distorted square pyramid; bis-bidentate (L1, L2) meds ligands: $\eta^{12}\mu_{10}$(L2): $\eta^6\mu_6$, $\eta^6\mu_6$ coord. modes; $\eta^{10}\mu_8$ (L1): $\eta^6\mu_6$, $\eta^4\mu_4$ coord. modes	chelate units via R1,2 (6); bis-chelate units via R2,4(8); catenating motifs: R2,2(4), R2,3(6)	Ag(1) square grids via R4,8(16) grids; Ag(2) chains via C1,2(6) and R2,3(6); 3D entanglement via R2,2(4), and R2,4(8) interweaving motifs.	[70]
71. catena-((μ_6-Ethane-1,2-disulfonato)-di-silver(i)) [Ag$_2$(1,2-etds)]$_n$	AGSLFA	$P\bar{1}$	Ag–octahedral, two close Ag-Ag distances; 1,2-etds: $\eta^{12}\mu_{12}$ ligand	Coord. monolayers (*ab*) formed via R1,2(4), R2,2(4), and R2,4(8) motifs	Pillared 3D network; aliphatic spacer between the monolayers are parallel	[71]
72. catena-((μ_{10}-Butane-1,4-disulfonato)-di-silver(i)) [Ag$_2$(1,4-buds)]$_n$	AGSLFB	$P2_1/c$	Ag–trigonal bipyramidal, one close Ag-Ag distance; 1,2-buds: $\eta^{10}\mu_{10}$ ligand	Coordination monolayers via R1,2(4) R2,2(4), and R2,4(8) motifs	Pillared 3D network; aliphatic spacer between the monolayers are interdigitated	[71]
73. catena-[(μ_8-η^2,η^2-1,5-Naphthalenedisulfonato)-di-silver(i)] [Ag$_2$(1,5-nds)]$_n$	GAKSOB	$P\bar{1}$	Ag–distorted tetrahedral; 1,5-nds: $\eta^{10}\mu_8$ ligand	Ag–sulfonate coord. layers: R2,4(8) linking motifs and R2,4(18) grids	Ag-η^{12}-arene interactions interlock the layers into porous 3D framework; alternating inorganic-organic regions	[72]
Complex salts						
74. catena-(Hexa-aqua-nickel (μ_2-25,26,27,28-tetrahydroxy-2,8,14,20-tetrathiacalix(4)arene-5,17-disulfonato-11,23-disulfonate)-bis(μ_2-aqua)-hexa-aqua-di-sodium) tetrahydrate	XAFFEQ	$P\bar{1}$	Ni–octahedral, Na1–octahedral	Ni-isolated coord. units; Na-2D coord. frameworks via R2,2(4) motifs	3D coordination networks	[73]

Abbreviations: meds = methanedisulfonate; 1,2-etds = ethane-1,2-disulfonate; 1,4-buds = butane-1,4-disulfonate; 1,2-bds = 1,2-benzenedisulfonate; 1,3-bds = 4,5-dihydroxybenzene-1,3-disulfonate; 1,3-ands = 6-aminonaphthalene-1,3-disulfonate; 2,6-ipds = 4-chloro-2,6-disulfono-methyl(imino)methyl)phenol; 1,5-nds = 1,5-naphthalenedisulfonate; 2,6-nds = 2,6-naphthalenedisulfonate; 2,7-nds = 2,7-naphthalenedisulfonate, peds = 4,4′-phenyletherdisulfonate; bpds = 4,4′-biphenyldisulfonate; 2,2′-bpy = 2,2′-bipyridine; en = ethylenediamine; *N*-meen = *N*-methylenediamine; *N*,*N*′-meen = *N*,*N*′-dimethylenediamine; 4-cyclam = 1,4,8,11-tetraazacyclotetradecane; 5-cyclam = 13-methyl-6-(1-phenylethyl)-1,4,6,8,11-pentaazacyclotetradecane; inia = isonicotinamide; pn = 2,3-diaminopropane; dien = diethylenetriamine; phen = phenanthroline, ABTS = 2,2-azino-bisN-ethylbenzothiazoline-6-sulfonate, 2,2-ambpds = 4,4′-diamino-5,5′-dimethyl-1,1′-biphenyl-2,2′-disulfonate.

[a] Structures assigned with asterisk are disordered.

[b] Structure omitted from the discussion (disordered sulfonate group).

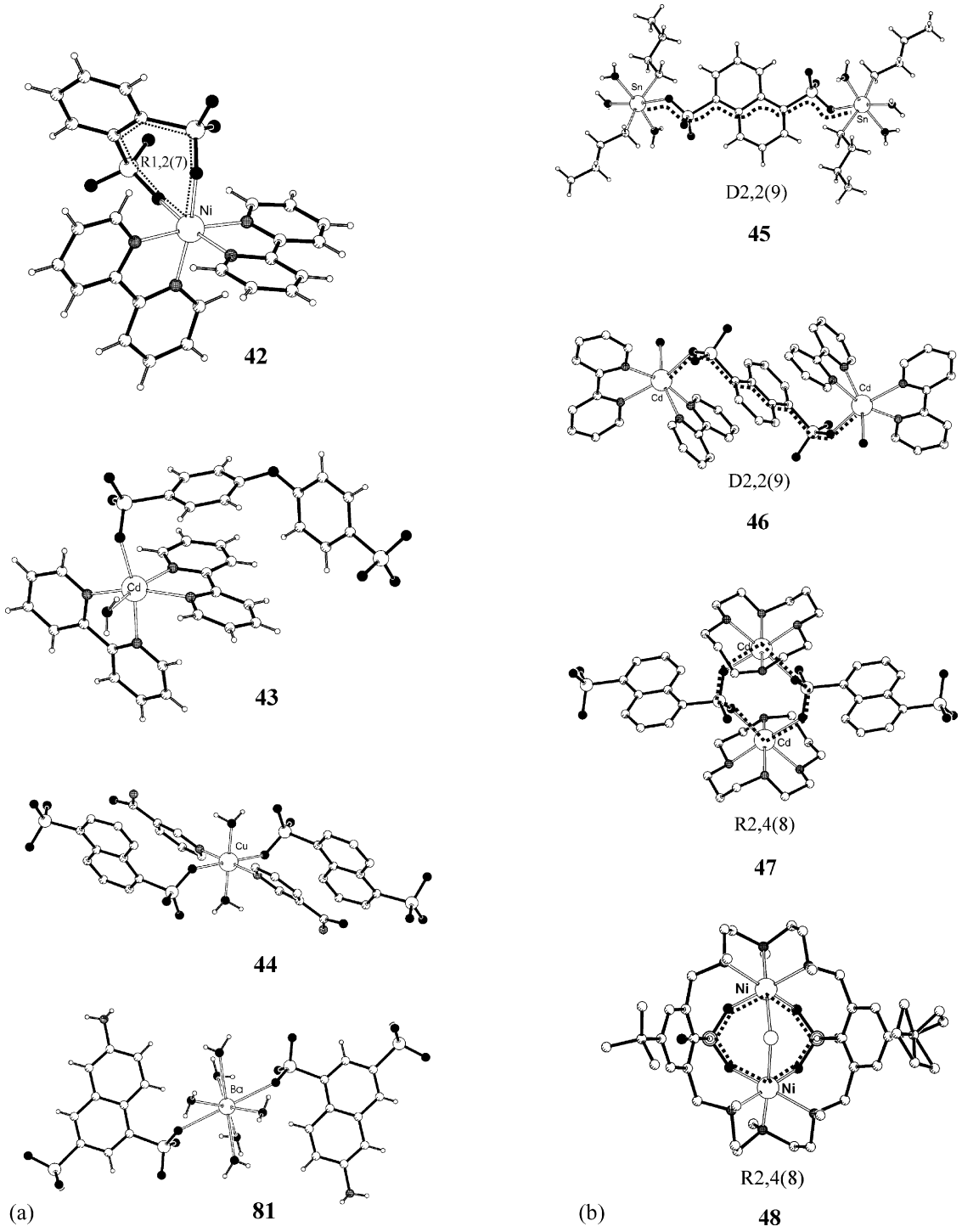

Fig. 2. (a) Presentation of isolated mononuclear coordination units. Each of the metal ligands binds the ion in a monodentate fashion (compounds **44** (Ref. [44]), **81** (Ref. [31])) or bidentate fashion, forming chelate ring(s) described with R1,2(*n*) (compounds **42** (Ref. [57]), **43** (Ref. [58])). (b) Presentation of isolated dinuclear coordination units described by two different coordination graphs: D2,2(*n*) denotes coordination units with a single ligand shared between the two metal centers; compound **45** (Ref. [59]) and **46** (Ref. [58]); R2,4(*n*) denotes cyclic dimers in which the metal centers share two common ligands (compounds **47** (Ref. [58]) and **48** (Ref. [60]).

toward both sulfonate sites of the meds ligands. However, the bulky substituents on the fifth, non-coordinated N-atom, tend to stay away from the cycloalkane ring and therefore align from one side of the chains. The entire crystal structure appears to be an interplay of three symmetry related (via three-fold rotation) coordination chains running along [1 0 0], [0 1 0] and [1 1 0] directions (Fig. 4).

Ten compounds (**52–62**, but not **54**) display similar 1D arrays. The topologically non-restricted sulfonate groups of the ligands bind crystallographically indistinguishable metal centers with a

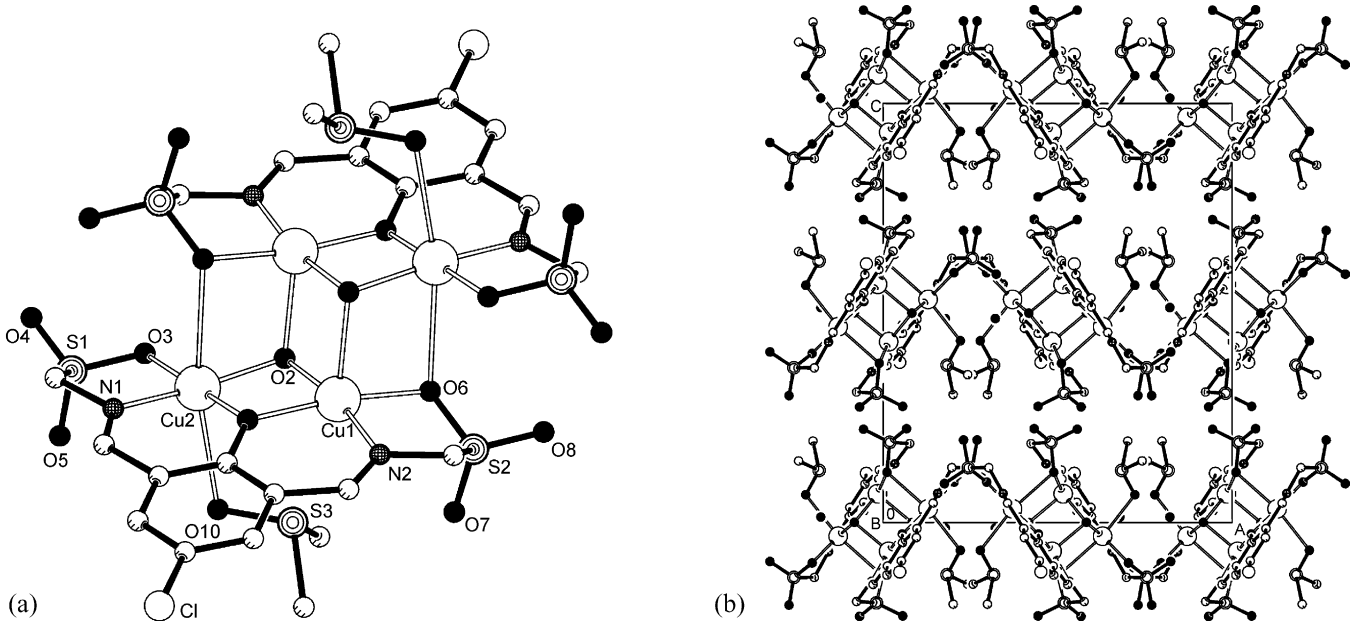

Fig. 3. (a) Presentation of the isolated tetranuclear coordination unit $[\{Cu_2(OH)(2,6\text{-ipds})\}(dms)]_2$ in **50** (Ref. [61]); (b) view down *b*-axis, showing the packing arrangement of the crystal. The coordination units are organized in monolayers and the hydration water (omitted in the picture) cross-links them in 3D.

$\eta^1\mu_1$ coordination mode in order to extend them into coordination polymers. The size of the R-spacer between the sulfonate groups dictates the distance between the metal centers. However, the geometry and the flexibility/rigidity of the R-spacers are crucial for the chain arrangement in the crystal. The auxiliary ligands significantly influence the relationship along and between the chains. The octahedral copper ions in **52** and **53** are extended into sinusoidal coordination chains C1,2(7) and C1,2(9), correspondingly. The metal centers along the chains are inversion related. The butane spacer in **53** allows for water–sulfonate interactions between neighboring reflection related [0 1 0] chains in order to form hydrogen bonded (1 0 2) monolayers, that are further hydrogen bond cross-linked into 3D. However, the short ethane spacer in **52** is not flexible enough to follow the symmetry requirements of the network, and hence, two independent chains Cu1 and Cu2, running along $[\bar{1}\ 1\ 0]$ direction, are formed. Mul-

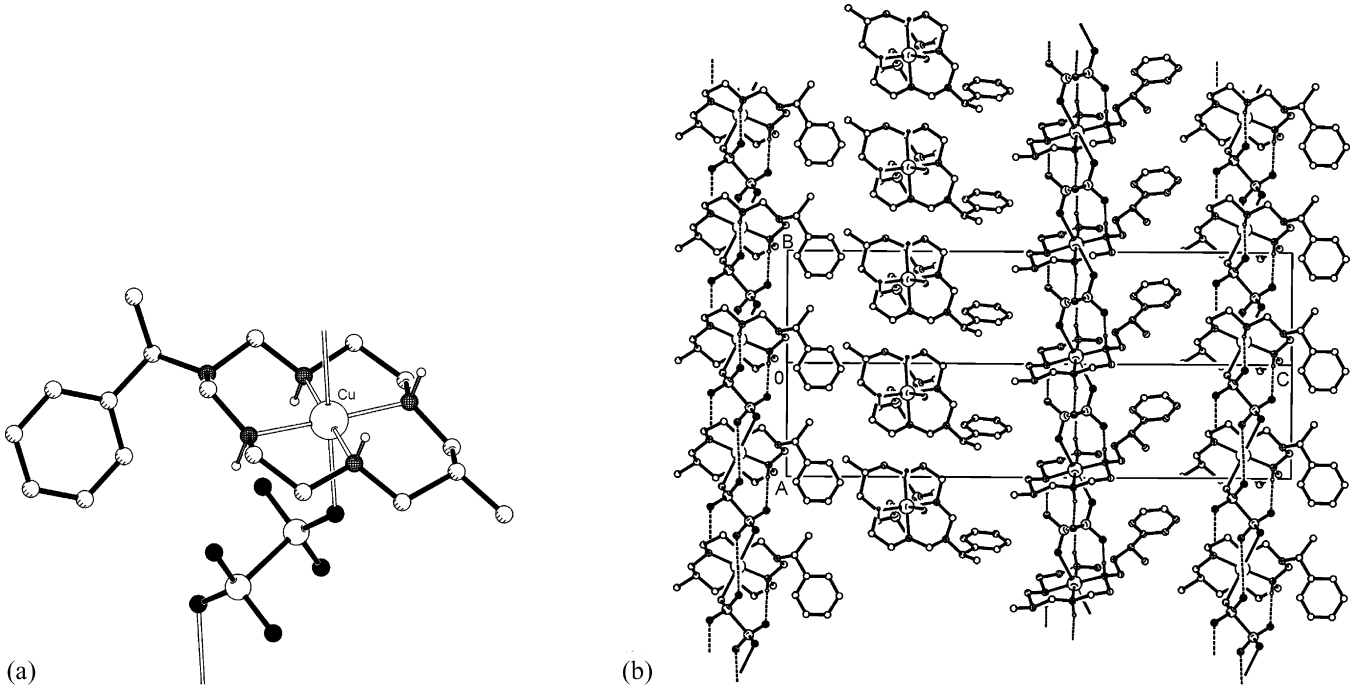

Fig. 4. (a) Presentation of the coordination unit [Cu(5-cyclam)(meds)] in crystal **51** (Ref. [62]); (b) the packing arrangement of the three symmetry related coordination chains. The hydrogen atoms, except those located on the coordinated N-atoms, are omitted.

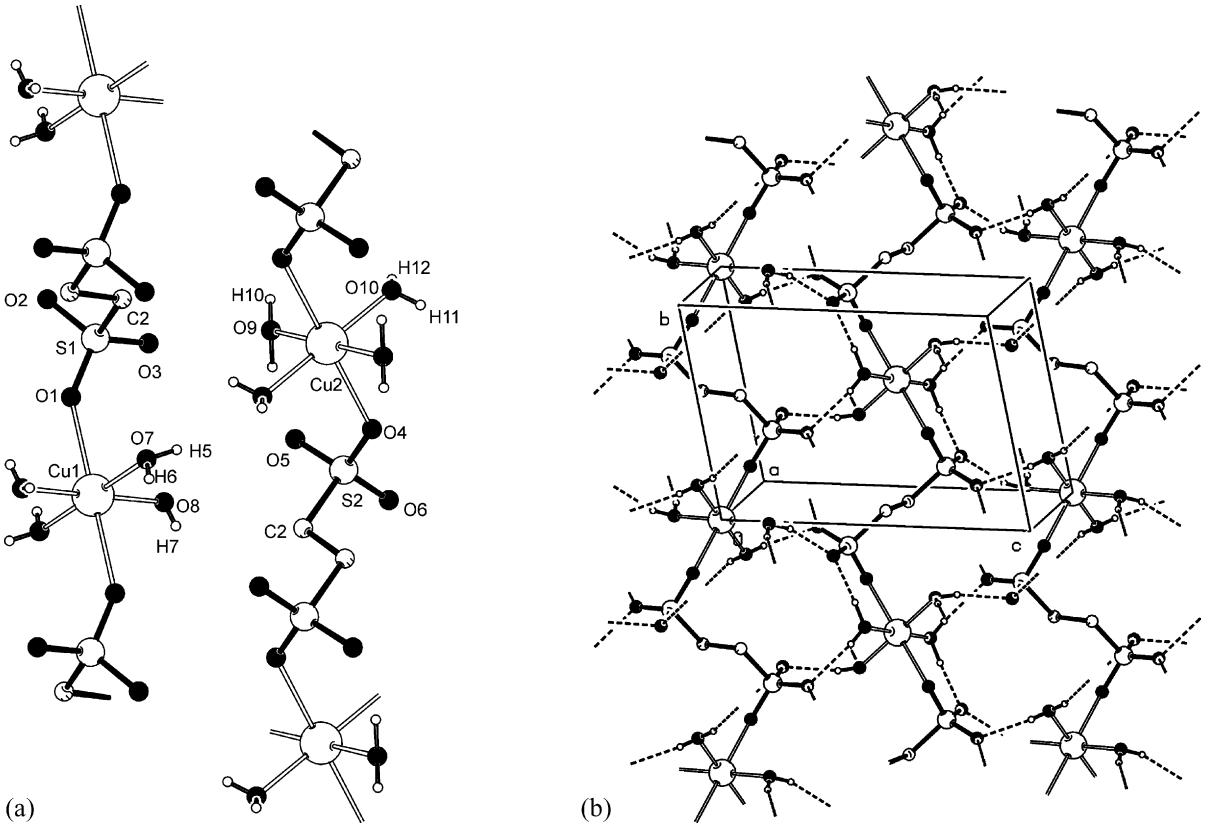

Fig. 5. (a) The symmetry independent coordination chains $[Cu(H_2O)_4(1,2\text{-etds})]_n$ in crystal **52** (Ref. [63]); (b) the formal hydrogen bonded monolayer (b).

tiple hydrogen bonds, donated from the aqua ligands toward the sulfonate groups, cross-link the chains into ($\bar{1}$ 1 1) monolayers and pack them into porous crystal network (Fig. 5).

Despite the fact that the geometry of 1,5-nds ligand in compound **54** allows for an inversion relationship between the metal centers, the impediments imposed by the triphenyl tin unit account for the different binding modes of the sulfonate groups. One of the sites bridges in $\eta^2\mu_2$ fashion the two independent $Sn1Ph_3$ and $Sn2Ph_3$ units, while the second site is coordinated only to Sn1 and serves to extend the screw related units into helical chains along the *b*-axis. The Sn1 centers in the helix are nine bonds apart (C1,2(9)), counted along the shortest pathway through C9–C10 bond (see Scheme 3). The $Sn2Ph_3$ units are attached in the folds of the Sn1 helices and adopt an optimal alignment with respect to the aromatic rings. Hydrogen bonds, donated from the Sn2 aqua ligand toward the $\eta^1\mu_1$ sulfonate site, join the neighboring translation related helices in order to form polar molecular layers. The naphthalene rings are embedded in the interior of the layer and the phenyl rings protrude into the interlayer region (Fig. 6). The relationships between the aromatic rings inside the layer are complicated, starting from face-to face (FF), through edge-to-face (EF) and T-shape arrangement. The solvated tetrahydrofuran molecules are intercalated between the Sn1 and Sn2 phenyl rings inside the monolayer. The monolayers are arranged in an anti-parallel manner with hydrophobic interactions dominating in the interlayer region. The 1,5-nds in **55** serves as an axial ligand and bridges the $[Cu(1,5\text{-nds})(py)_4]$ units into [1 1 $\bar{1}$] zig-zag chains. For geometrical reason the pyridine rings of the species are oriented perpendicular to the equatorial plane of the coordination unit. The repulsion effects between the coordination sites and the lack of stabilizing hydrogen bond donors lead to dynamical disorder of the sulfonate groups. The cyclam moiety in $[Ni(4\text{-cyclam})(1,5\text{-nds})]_n{\cdot}nH_2O$ **56** serves as a tetradentate ligand and forms four coplanar chelate rings (two (R1,2(6) and two R1,2(5) motifs). The 1,5-nds ligand bridges the Ni-cyclam units into a C1,2(9) chain which is additionally strengthened by intrachain hydrogen bonds (N–H$\cdots$O(S)), established between the cyclam and 1,5-nds ligands. Despite the bulkiness and rigidity of the spacer in 1,5-nds, the distance between the metal centers is the same as in **53** (see Scheme 3). For reasons of dense packing in the crystal network and geometrical requirements of the cyclam ligand, the chains are forced to run in two different, symmetry related [1 1 0] and [1 $\bar{1}$ 0] directions. Crystalline water cross-links the chains in order to form a porous hydrogen bonded 3D network. The cyclam ligands are arranged in the square channels generated along the *c*-axis (Fig. 7).

The auxiliary ligands in $[Cd(N,N'\text{-meen})_2(1,5\text{-nds})]$ **57** chelate the metal ion with two rings R1,2(5). The bridging 1,5-nds ligand extends the chelate units into C1,2(9) arrays along [1 $\bar{1}$ 0] direction. The *N*-methyl substituents in *N*,*N*′-meen adopt an equatorial orientation versus the plane of the chelate ring. This allows the axially oriented amino hydrogen atoms to approach the sulfonate oxygen atoms of the neighboring chains in order to form hydrogen bonded (*ab*) monolayers (Fig. 8a). Both, the coordination rings R1,2(5) and the naphthalene rings are ori-

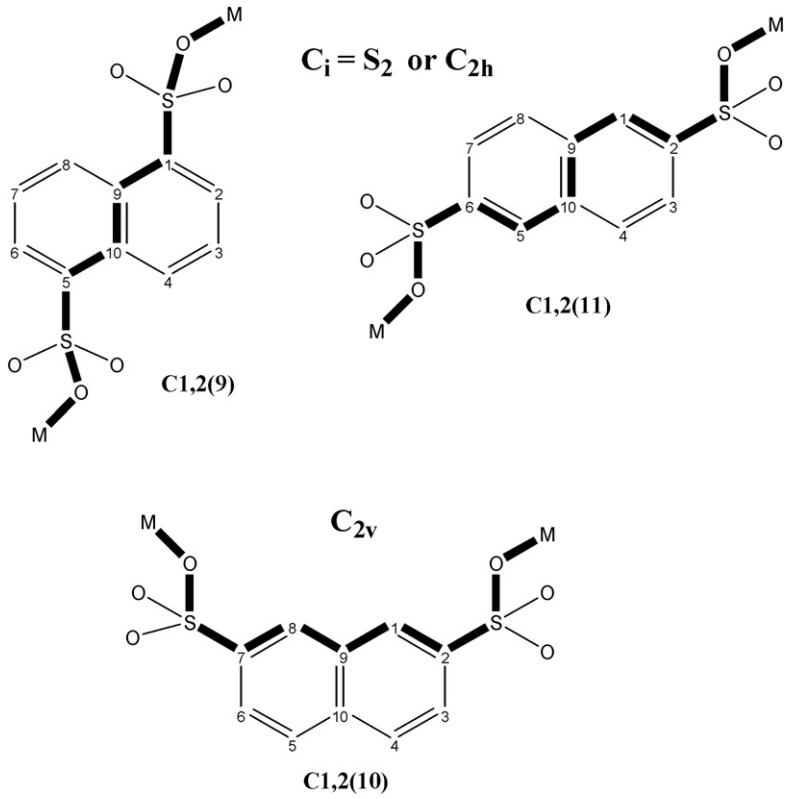

Scheme 3.

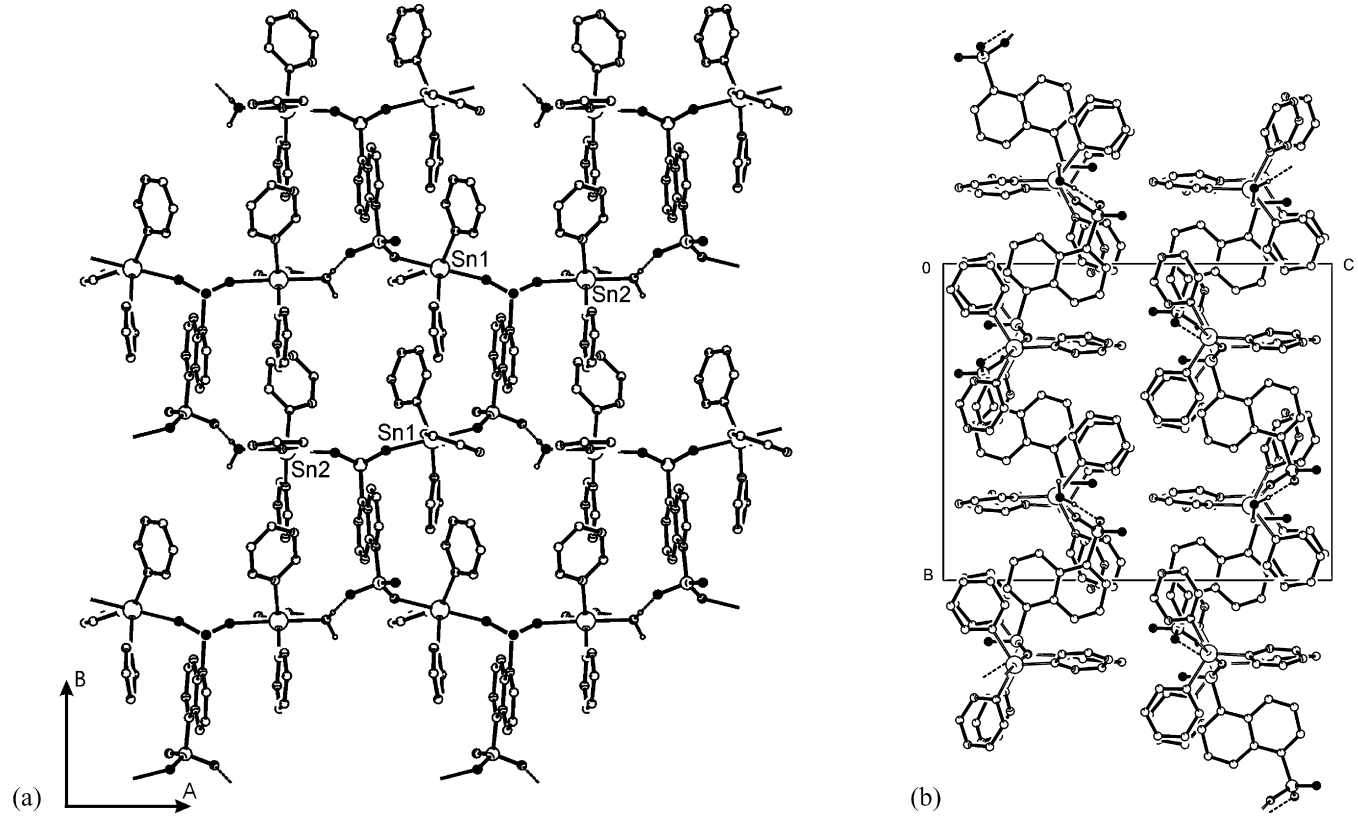

Fig. 6. (a) The 1D coordination extension in crystal **54** (Ref. [64]) are helical and align parallel in order to form polar hydrogen bonded monolayers; (b) the side view of two neighboring monolayers shows the hydrophobic interlayer region. For the sake of clarity the solvate tetrahydrofuran molecules are omitted.

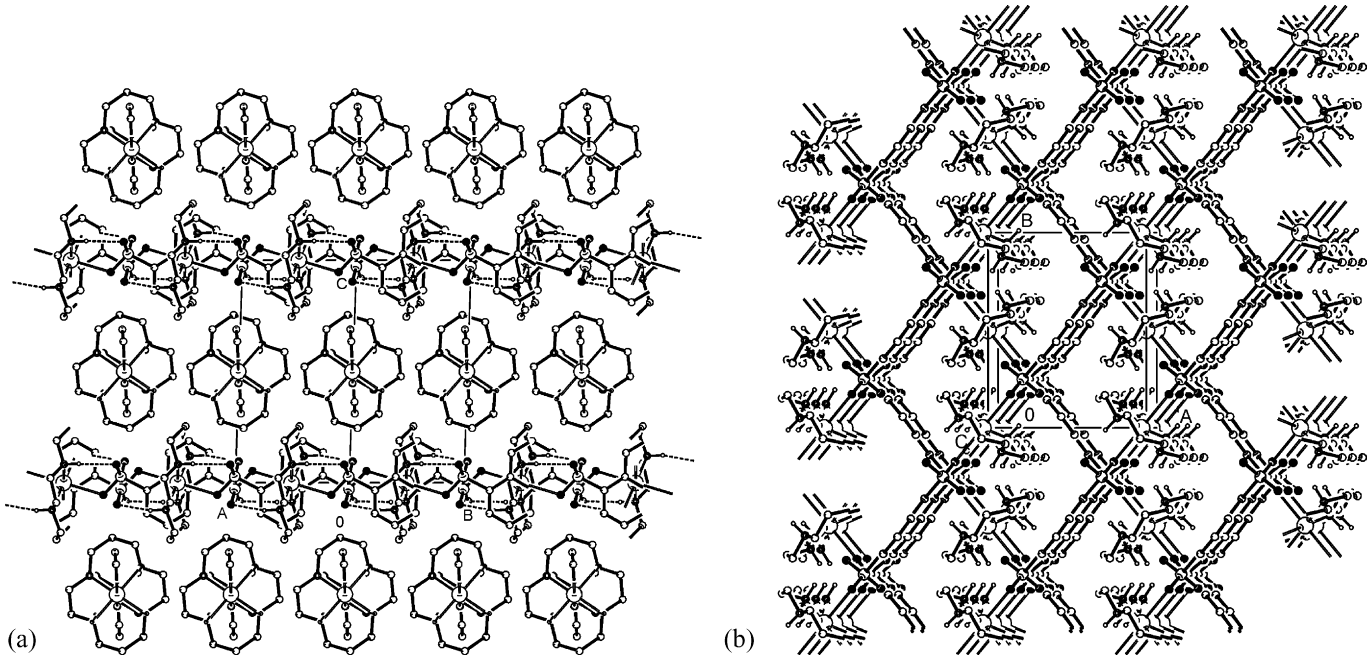

Fig. 7. The crystal arrangement in compound **56** (Ref. [43]) viewed along [1 1 0] and [0 0 1] directions. (a) The one-dimensional coordination extensions [Ni(4-cyclam)(1,5-nds)]$_n$ propagate in two different symmetry related directions. (b) The chains are interlocked via the crystalline water (omitted in the picture) into a supramolecular structure with cyclam ligands arranged in the square channels formed along the *c*-axis.

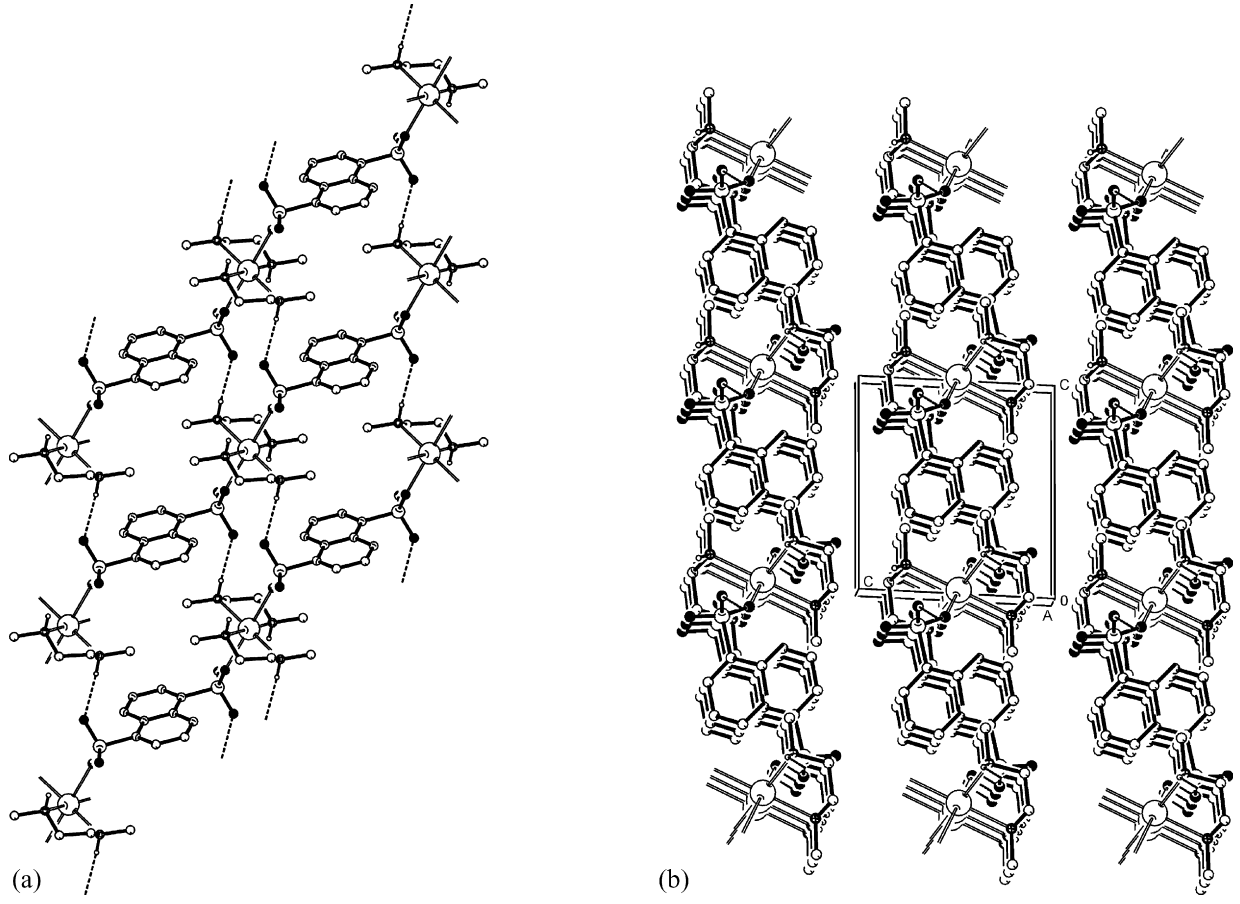

Fig. 8. (a) The hydrogen bonded monolayer [Cd(*N*,*N*′′-meen)$_2$(1,5-nds)]$_n$ in compound **57** (Ref. [65]); (b) the packing arrangement of the monolayers. All hydrogen atoms of the ligands, except H(N), are omitted.

ented almost perpendicular versus the mean plane of the layer and arranged in stacks along the [1 0 1] direction which makes the monolayer thick. There are no interactions between the aromatic portions inside the layer. The methyl groups of the *N*,*N*′-meen ligands protrude into the interlayer region where the hydrophobic interactions are predominant (Fig. 8b).

The topology of the coordination sites in the aromatic spacer is also important for the structural organization (see Scheme 3). The distance between the metal centers in the 1D array lengthens from 9 to 11 bonds upon changing 1,5-nds for 2,6-nds ligand (compounds **58**–**61**). The coordination species $[Cd(N,N'\text{-meen})_2(2,6\text{-nds})]_n$ in **58** differs from that in **57** only in interdistance between the Cd ions. However, the 3D arrangement of the chains significantly changes. The *N*-methyl groups of the auxiliary ligand are forced to adopt an axial conformation, in order to escape crowding with the 2,6-nds ligand. In consequence the sulfonate oxygen atoms of the chain became accessible for the equatorial amino protons in order to form intrachain instead of interchain hydrogen bonds This prevents the formation of monolayers in **58** and the crystal packing of the coordination arrays takes place with the generation of hydrophobic regions where the (axial) methyl groups are embedded (Fig. 9). The individual coordination unit $[Cd(N\text{-meen})_2(2,6\text{-nds})]$ in compound **59** is very similar to that in **58**. However, due to the lower symmetry of the auxiliary ligand (as compared to that of *N*,*N*′-meen), the 1D arrays run in two different directions [1 1 0] and [1 $\bar{1}$ 0]. The single methyl group of *N*-meen adopts an equatorial position versus the chelate rings of the system. The different orientation of the amino hydrogen atoms (two N–H bonds are axial and one is equatorial) allows for amino-sulfonate interactions between the coordination arrays. Neighboring *a*-translation related chains are hydrogen bonded via the $N\text{–}H_{axial}\cdots O$ in order to arrange in screw related molecular monolayers alternating along [0 0 1] direction (Fig. 10a). The chelate and the naphthalene rings align almost perpendicular to the mean layer plane. The two methyl groups of the chelated unit are also embedded in the intralayer region, while the third sulfonate oxygen, not employed in the layer formation, protrudes into the interlayer region. This makes the interior of the monolayer hydrophobic and the exterior hydrophilic and

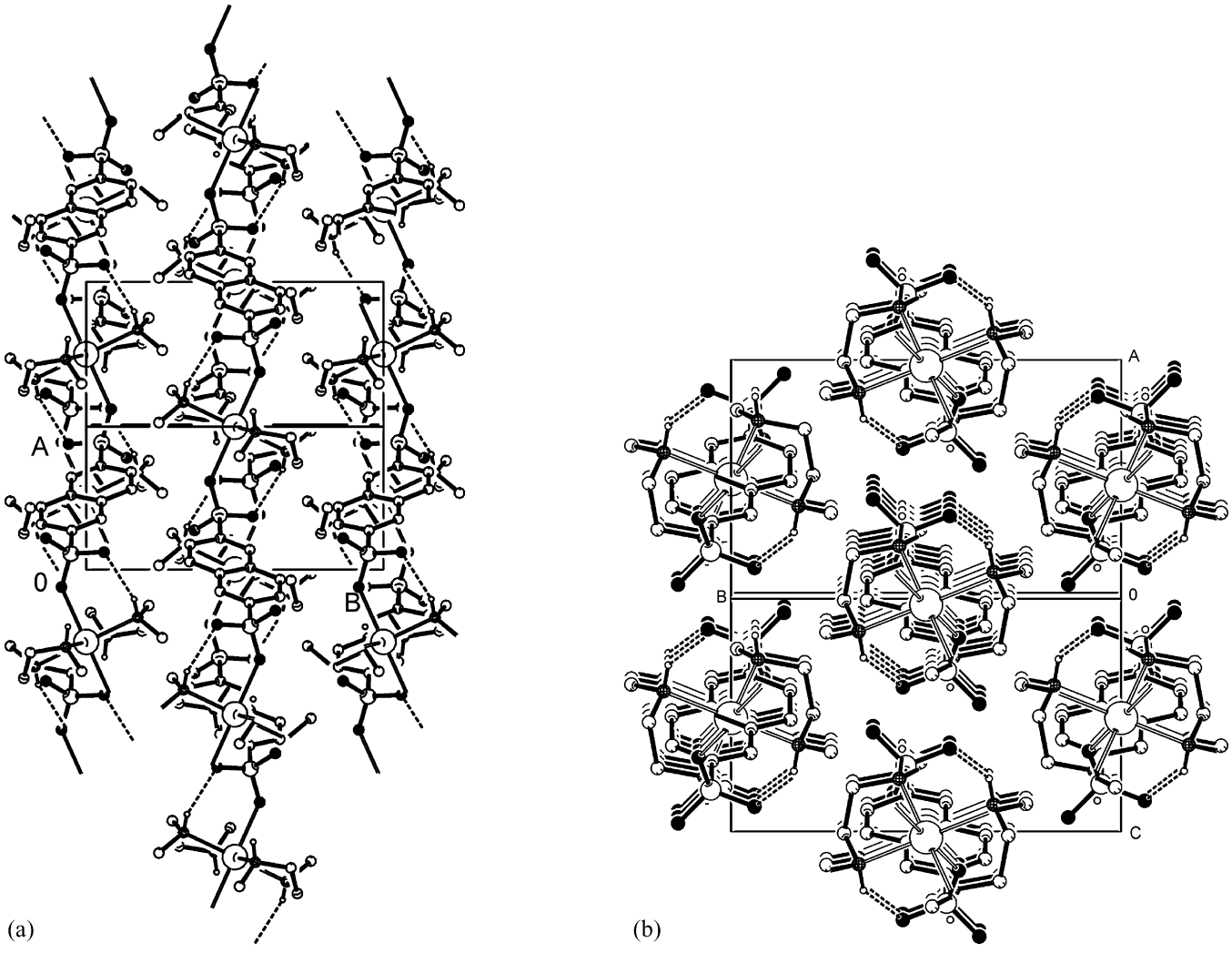

Fig. 9. The 1D coordination arrays $[Cd(N,N''\text{-meen})_2(2,6\text{-nds})]_n$, in **58** (Ref. [65]) propagate along the [1 0 1] direction (a) and align in an anti-parallel manner with hydrophobic interactions between them (b). All hydrogen atoms, except H(N), are omitted.

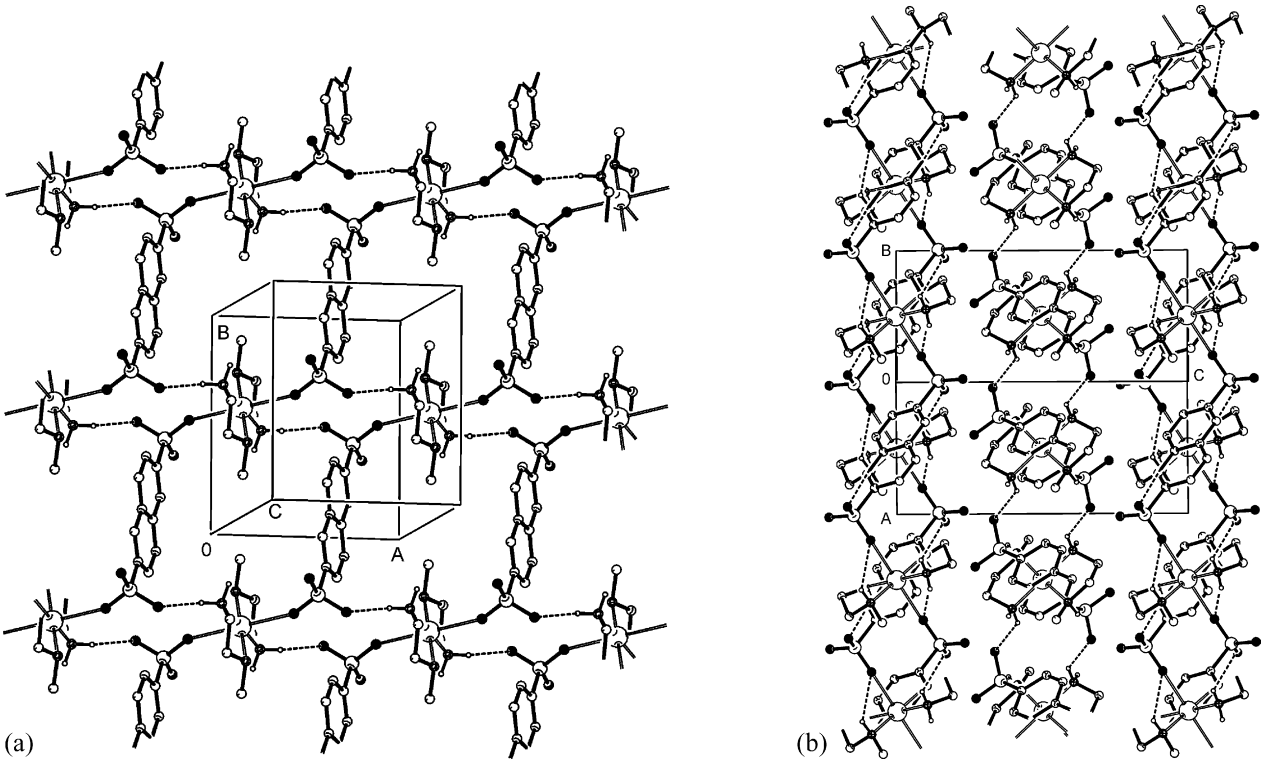

Fig. 10. (a) The 1D coordination arrays $[Cu(N\text{-meen})_2(2,6\text{-nds})]_n$, **59** (Ref. [65]), are interlinked (via $N–H_{axial}\cdots O(S)$) into hydrogen bonded monolayers; (b) the packing arrangement of the monolayers. For the sake of clarity the crystal water molecules which hydrogen bond the monolayers are omitted.

the water molecules, arranged between the monolayers serve to cross-link them via $O_w–H\cdots O(S)$ and $N–H_{equatorial}\cdots O_w$ hydrogen bonds. The copper analogous $[Cu(N\text{-meen})_2(2,6\text{-nds})]_n\cdot 2nH_2O$ **60** is isostructural with **59**. The auxiliary ligands in $[Cd(inia)_2(H_2O)_2(2,6\text{-nds})]_n\cdot 4nH_2O$ are monodentate and do not introduce geometrical or steric restrictions to the species. The flexibility of the sinusoidal coordination chain C1,2(11) in **61** allows for a porous supramolecular arrangement. Coordination water–sulfonate hydrogen bonds link the inversion related chains in order to form monolayers (0 1 $\bar{1}$), with big holes, described by $R_2^2(12)$, and $R_2^2(26)$ hydrogen bonded motifs. The inia ligands, are arranged from both sides of the monolayers and approach the neighboring monolayers via an amide–sulfonate hydrogen bond, in order to furnish the 3D network. The alignment of the aromatic portions of the ligands takes place with edge-to-face (EF) interactions between the pyridine and naphthalene rings along the chains and face-to-face (FF) interactions between the naphthalene rings inside the monolayers. The crystalline water is arranged in the big channels generated along [1 0 0] direction and serve to stabilize the crystal structure via additional hydrogen bonds.

The disulfonate R-spacer used in compounds **62–65** is longer and has some rotation flexibility. The bridging bpds ligand extends the metal centers into C1,2(13) coordination polymer. However, the auxiliary ligands can effectively change both the symmetry relationships along the 1D arrays and the packing patterns in these crystals. Two symmetry operators are imposed along the [1 0 1] chains in $[Cu(dapn)_2(bpds)]_n$ **62**:$\bar{\mathbf{1}}$(at the Cu-center) and **2** (in the C–C midline between the phenyl rings). Multiple inter-chain amino–sulfonate hydrogen bonds furnish the supramolecular network of the crystal. The structural arrangement of $[Cd(N,N'\text{-meen})_2(bpds)]$ in crystal **63** is similar to that of $[Cd(N,N'\text{-meen})_2(1,5\text{-nds})]$ in **57**. The coordination chains are further hydrogen bonded into (0 1 1) monolayers, but the size of windows are bigger (30-membered hydrogen bonded rings in **63** versus 22-membered in **57**). The phenyl rings are oriented perpendicular to the plane of the monolayer, and stacked at *a*-distance one from another. The *N*-methyl groups protrude into the monolayers and are arranged between them. The solid state organization of compound $[Cd(inia)_2(H_2O)_2(bpds)]_n\cdot 4nH_2O$ **64** is identical with that of $[Cd(inia)_2(H_2O)_2(2,6\text{-nds})]_n\cdot 4nH_2O$ **61** and the crystals are isostructural. The only difference is the size of the intra- and interlayer hydrogen bonded motifs, generated by the coordination water–sulfonate and amide–sulfonate interactions, correspondingly.

The basic building unit of compound **65** is dinuclear and described by a D2,2(14) coordination motif. Both Cd1 and Cd2, are octahedral, but the lack of symmetry between the aromatic rings of bridging peds ligand makes them distinguishable and their coordination environment is different. Cd2 is coordinated by two inia, two aqua and two peds ligands, while Cd1 by two inia, one aqua and three peds, one of which is shared with Cd2. The two peds ligands of the system also coordinate in a different manner. One of them, peds1, exploits only one of its sulfonates group as a coordination ligand and links in $\eta^2\mu_2$ fashion the Cd1 centers of neighboring, inversion related D2,2(14) units. On the other hand, peds2 is shared between Cd1 and Cd2 of the basic unit D2,2(14) and additionally bridges the Cd2 centers

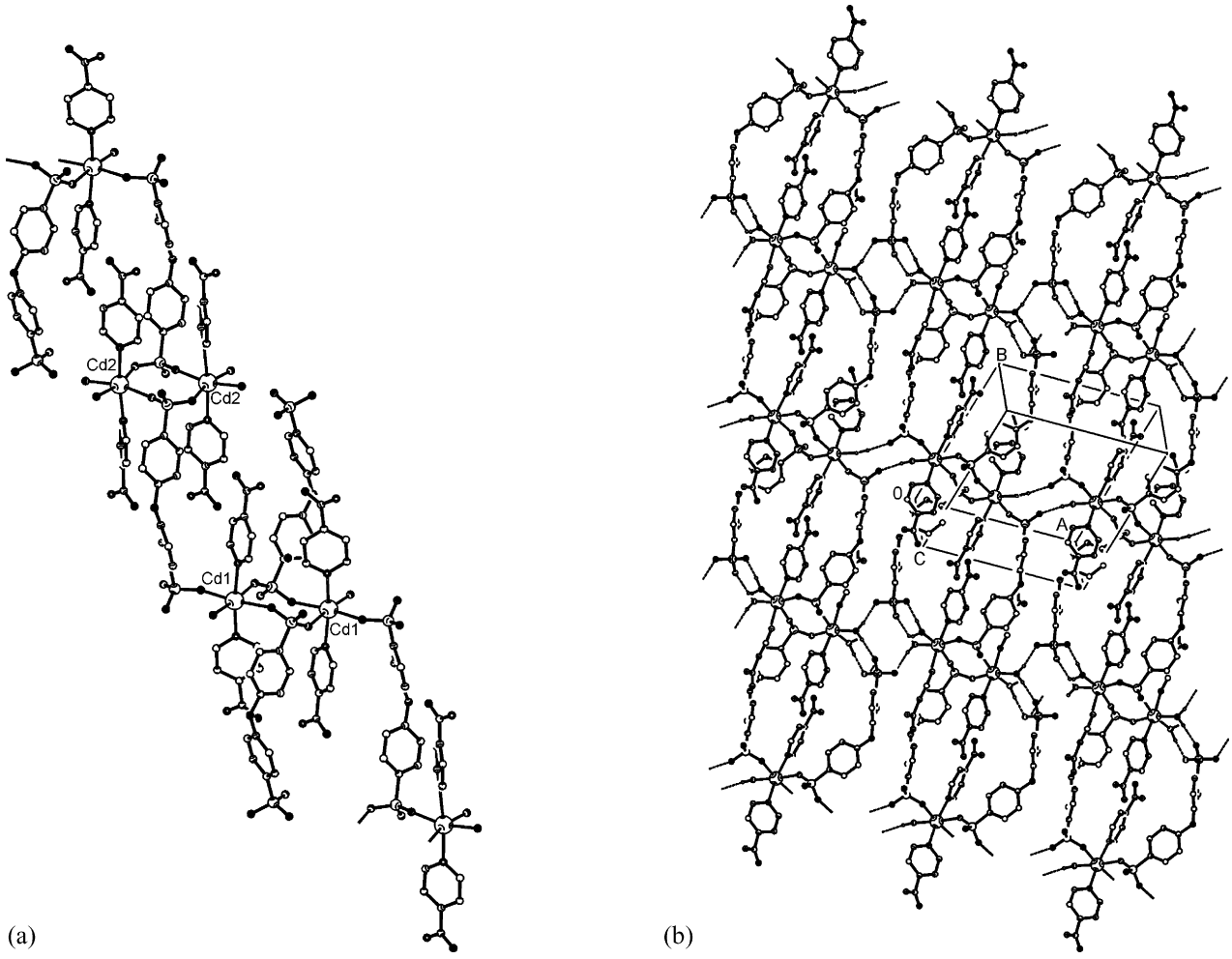

Fig. 11. The coordination ribbon $[Cd_2(inia)_4(H_2O)_3(peds)_2]_n$ (a) and the hydrogen bonded monolayers; (b) in crystal **65** (Ref. [58]).

of neighboring units with $\eta^2\mu_2$ mode. Therefore, the different linking motifs R2,4(8) are formed on both ends of D2,2(14) units: Cd1–Cd1 via sharing of two peds1 and Cd2–Cd2 via two peds2 ligands. The extended 1D array propagates along [0 $\bar{2}$ 1] direction. The periodic distance between the metal centers along the polymeric ribbon is C3,4(28) (see Fig. 11a). The two phenyl rings of peds are twisted almost perpendicular and variable aromatic interactions take place in the crystal. There is a plethora of hydrogen bonds established between the amide hydrogen atoms, and the sulfonate and aqua oxygen atoms. Hydrogen bonds, established between the aqua ligands and the sulfonate oxygen atoms, not involved in coordination bonds, join neighboring ribbons (via $R_2^2(12)$ and $R_4^4(14)$ motifs) in order to form (0 $\bar{1}$ 2) monolayers (Fig. 11b). On the other hand, amide–sulfonate hydrogen bonds cross-link the monolayers into 3D supramolecular network. Two crystalline water molecules are incorporated in the interlayer region and additionally stabilize the crystal structure.

7.3. Two-dimensional coordination networks

At least two oxygen atoms belonging to the same sulfonate site should be involved in coordination bonds in order to extend the coordination units in two-dimension. Only four disulfonato transition metal ion complexes **66–69** display 2D coordination network. Three of them are cadmium and the fourth one is a lead compound.

The usual coordination geometry of cadmium ion is octahedral. However, the methanedisulfonate compound Cd^{2+} demonstrates preferences for seven-coordination with a pentagonal bipyramidal geometry and crystals **66** and **67** appear to be two different polymorphic forms of cadmium methanedisulfonate trihydrate. Three methanedisulfonate (meds) and three aqua ligands penetrate the first coordination sphere of the metal ion. Due to the short (two bonds') distance between the sulfonate sites, the meds ligand is predisposed for bidentate metal binding. So, two sulfonate oxygen atoms, belonging to both ends of meds, donate electron pairs toward the same metal ion forming a R1,2(6) chelate ring. Two other oxygen atoms of each site serve to interlink the chelate units via bonds donated toward neighboring metal centers. So, the whole disulfonate moiety acts as $\eta^4\mu_3$ ligand and bridges three symmetry related Cd^{2+}, which leads to entanglement of the individual coordination motifs in two dimensions. In crystal **66**, one of the sulfonate groups is used to extend the chelate units into 1D coordination chains along *a*-direction (Fig. 12a). The second sulfonate group interweaves the

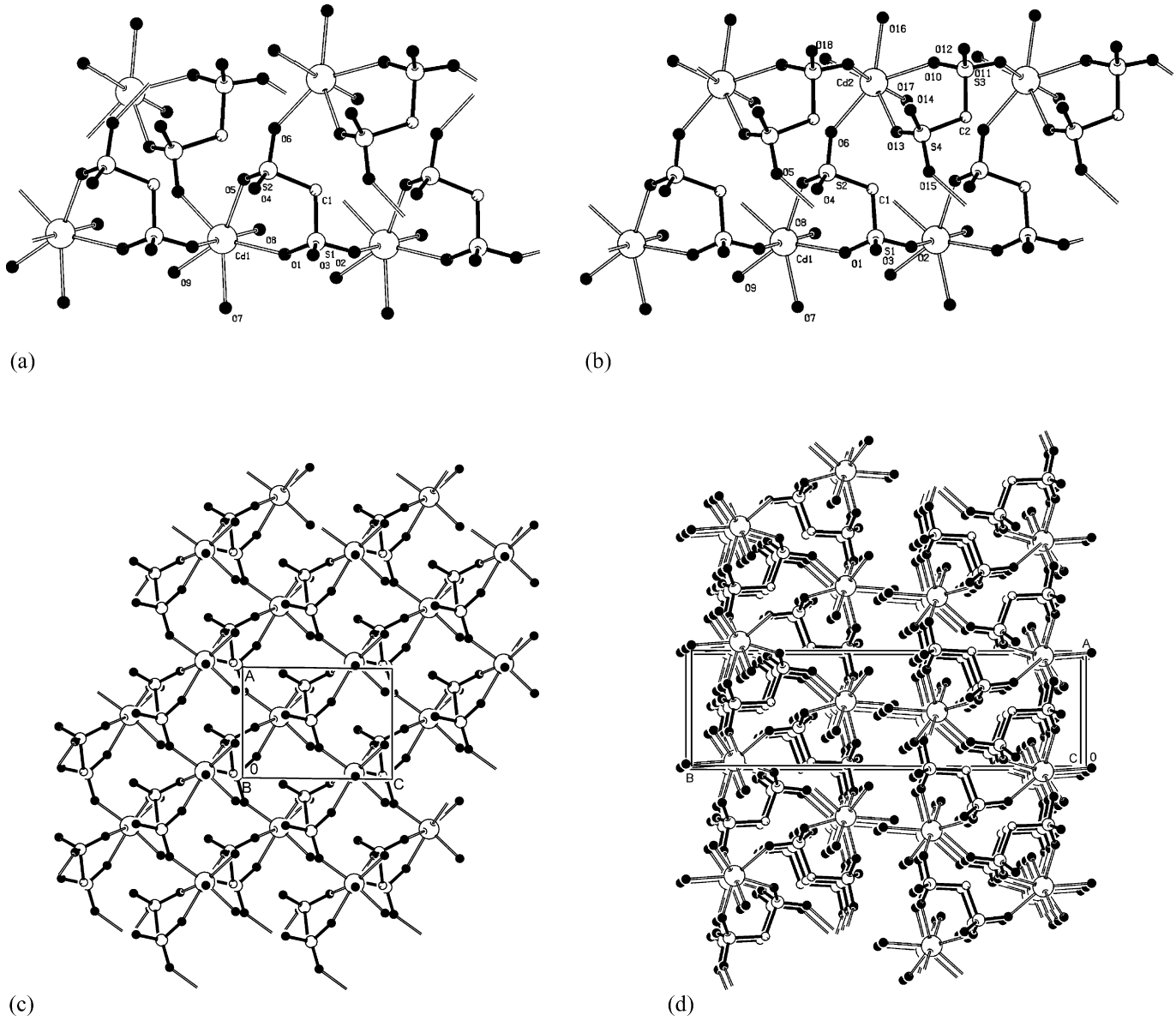

Fig. 12. The coordination species $[Cd(H_2O)_3(meds)]$ (a) and $[Cd_2(H_2O)_6(meds)_2]$ (b); a view of the monolayer (c) and a side view of two monolayers (d) in crystal **66** (Ref. [67]). The intra- and interlayer hydrogen bonds are not shown in the pictures.

glide related chains into wavy 2D coordination frameworks with R3,6(14) windows closed between three metal centers (Fig. 12c). The hydrogen bonds established between two of the aqua ligands and the sulfonate groups furnish the final architecture of the 2D array forming a thick (*ac*) monolayer. The sulfonate moieties are arranged in the interior of the monolayer and the metal ions on its surfaces. The third aqua ligand protrudes into the monolayer and donates hydrogen bonds toward one of the sulfonate groups of the next inversion related monolayer (Fig. 12d). The chelate units and the linking modes used for two-dimensional extension in the polymorphic crystal **67** are the same as in **66**. However, the glide relation between the 1D arrays is lost and therefore the two-dimensional framework in **67** appear to be an interplay of two symmetry independent Cd1 and Cd2 coordination chains. The hydrogen bonds inside the monolayers and between them are similar to those in **66**. The lack of a symmetry relationship between the chains in the monolayer leads to lowering of the crystal symmetry from $P2_1/n$ to $P\bar{1}$. So, the crystals **66** and **67** appear to be two supramolecular isomers of the same compound.

The tetranuclear cadmium compound $[Cd_4(H_2O)_8(1,5\text{-nds})_4]_n$ **68**, space group $P\bar{1}$, also displays a monolayer structure. Each sulfonate groups of 1,5-nds, serves as an equatorial ligand and bridges the Cd ions in $\eta^2\mu_2$-fashion in order to form a coordination monolayer. The aqua ligands are in axial position versus the mean plane of the monolayer and serve to hydrogen bond the monolayers. However, the preferences of the Cd ions for four equatorial 1,5-nds ligands in the first coordination sphere barely fulfill the symmetry demands of the coordination species and the crystal lattice. This leads to differentiation of the metal centers. A reasonable way to disentangle the 2D coordination framework

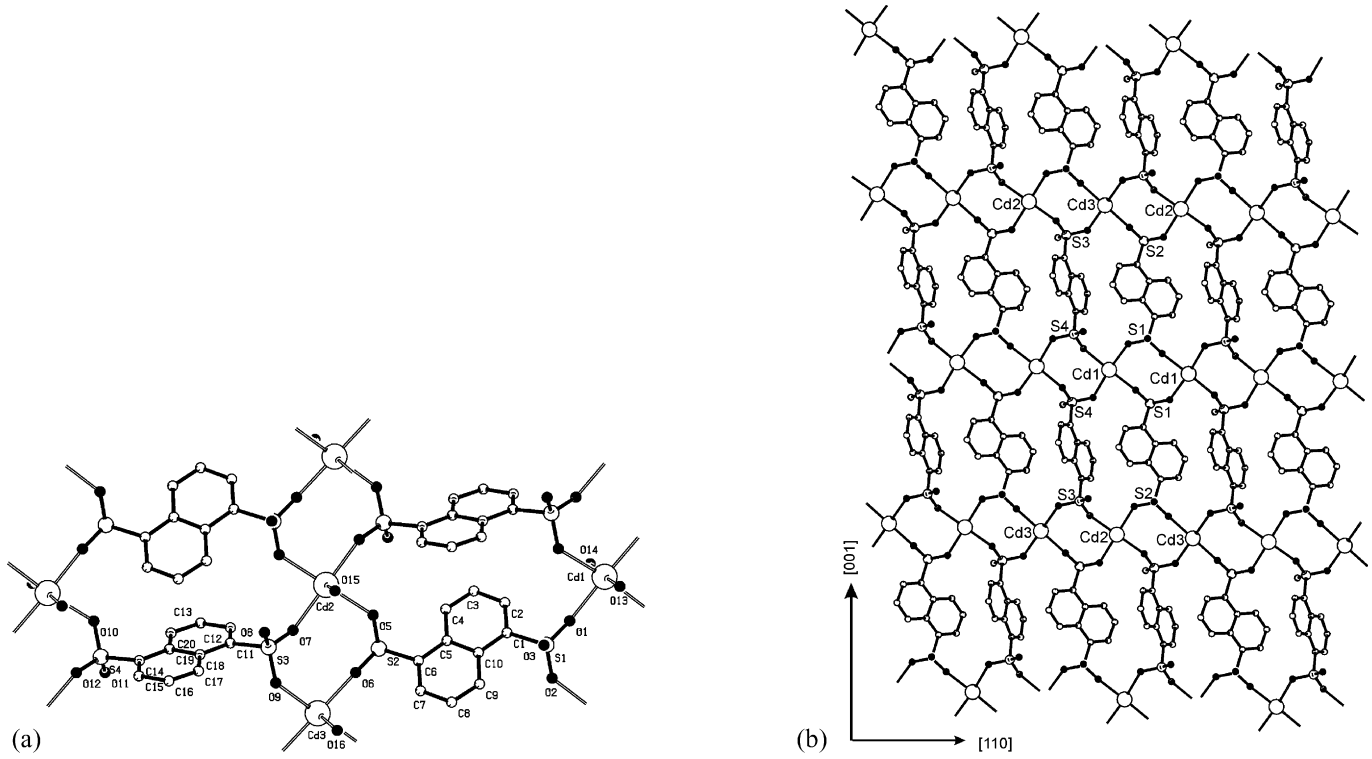

Fig. 13. The tetrameric coordination unit $[Cd_4(H_2O)_8(1,5\text{-nds})_4]$ (a) and the 2D coordination network (b) in compound **68** (Ref. [58]). All hydrogen atoms and the aqua ligands are omitted.

is to consider the two-dimensional intertwining of coordination dimers. Two 1,5-nds ligands are shared between Cd1 in order to form a centrosymmetric R2,4(8) coordination dimer. Two other 1,5-nds ligands, coordinated to the Cd1 centers, serve to extend the dimers into 1D ribbon arrays via another R2,4(8) motif. Two more ions (Cd2 and Cd3) are used to interlock the opposite sulfonate sites of Cd1–Cd1 ribbons in order to furnish the 2D coordination framework. The bulky aromatic linkers between the ribbons should subordinate both the coordination configuration of the metal ions and the symmetry requirements of the network. However, for geometrical and space reasons the naphthalene rings are forced to incline versus the mean plane of the monolayer, which leads to breaking of the local symmetry and differentiation of the ligands and the metal centers. Therefore, no symmetry element is imposed on the Cd1 centers and the inversion relation along the Cd1–Cd1 ribbon is not operative between the ligands, but it is operative between the metal centers. The intertwining motifs R2,4(8) are centrosymmetric and alternate along the ribbon with a periodic distance of C3,4(8). This leads to differentiation between the metal ions (Cd2 and Cd3), used to interlock the opposite sulfonate sites of Cd1–Cd1 ribbons. Both Cd2 and Cd3 lie on inversion centers, while the interlocking motif R2,4(8) is non-centrosymmetric (see Fig. 13). Therefore, the final coordination species consists of four metal ions, which share four different, but pair-wise symmetry related 1,5-nds ligands and the observed entanglement is a consequence of compromises between symmetry requirements and close packing demands of the network. The ligand spacers are arranged between the coordination ribbons and align with edge-to-face (EF) interactions between neighboring naphthalene rings. Interlayer aqua–sulfonate hydrogen bonds furnish the 3D supramolecular network. The overall crystal structure is featured by organic and inorganic regions alternating along the *c*-crystal axis.

7.4. Three-dimensional coordination networks

Only four of the retrieved structures (**70**–**73**) display three-dimensional coordination arrays and they all belong to silver(I) compounds. Compound $[Ag_4(meds)_2]_n$, **70**, crystallizes with a polar $Pmc2_1$ space group. The metal-ligand combination of labile silver ions and meds ligands, predisposed for bidentate binding, results into unique interweavement of coordination units in order to form a polythreaded network. There are two different bis-bidentate meds ligands L1 and L2 and two symmetry independent metal ions Ag1 and Ag2 with different coordination geometry. The coordination sphere of Ag1 ion is penetrated by five meds ligands forming one bidentate and four monodentate bonds. The Ag2 ion is five-coordinate with one bidentate and three monodentate bonds donated from four meds ligands. Each of the meds ligands binds in a bidentate fashion to two reflection related metal ions in order to form a bis-chelate coordination unit with R2,4(8) motif. The two different bis-chelate units, Ag2–Ag2 formed by L1 and Ag1–Ag1 formed by L2, can be considered as basic building units of the crystal. The units are extended into two different coordination rods along the *b*-direction, making use of new R2,4(8) motifs (Fig. 14a). Both sites of L2 adopt $\eta^6\mu_6$ coordination modes in order to

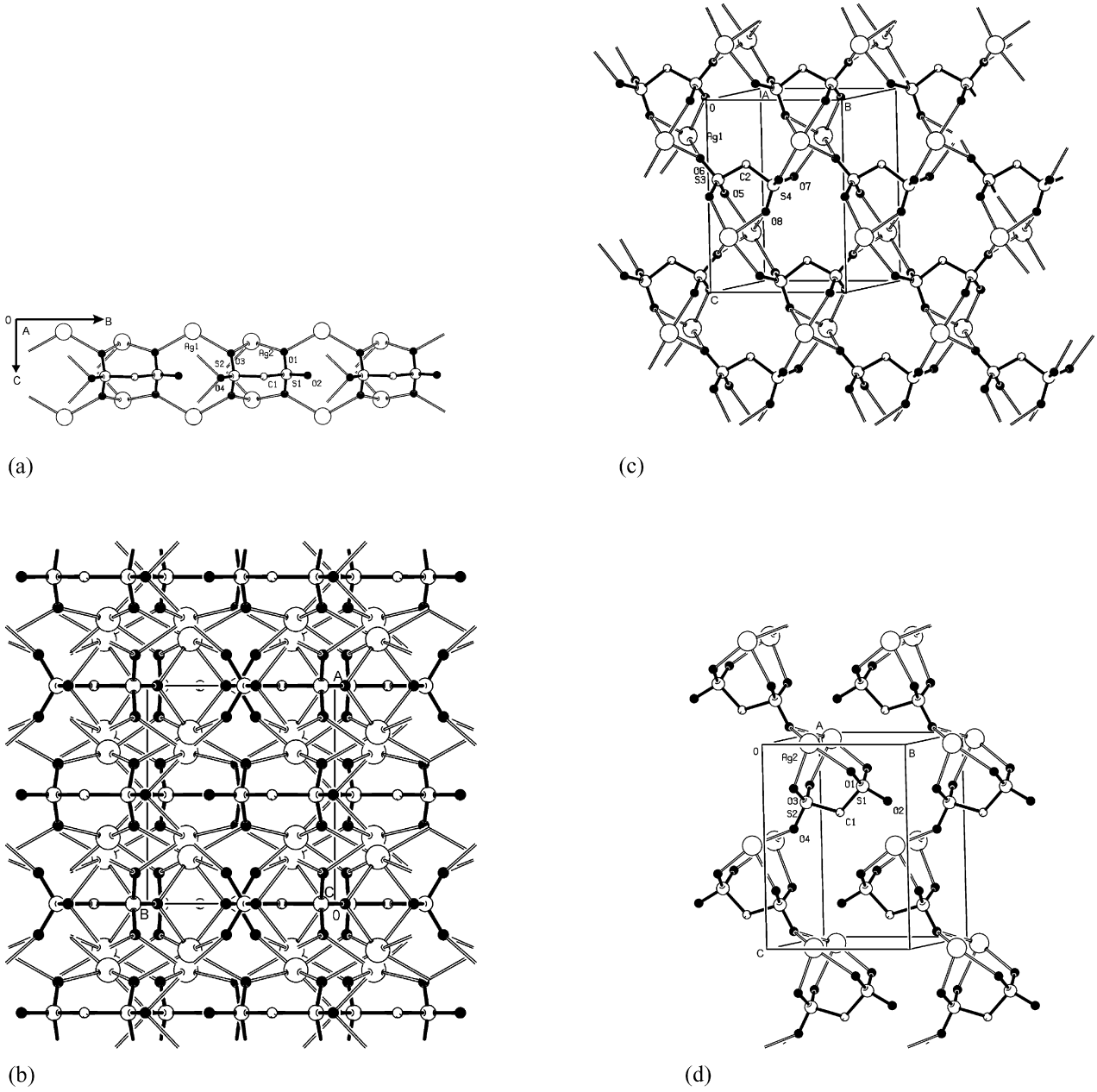

Fig. 14. (a) The one-dimensional extension of bis-chelate coordination units, giving coordination rods Ag1–Ag2–L1. The 3D coordination network $[Ag_4(meds)_2]_n$ in **70** (Ref. [70]) can be considered as: an interweavement of Ag1–Ag2–L1 and Ag1–Ag2–L2 coordination arrays, catenated via numerous Ag1–Ag2 R2,2(4) motifs (b); or as interpenetration of two independent Ag1–L2 and Ag2–L1 frameworks (c and d), that are interlocked via Ag1–Ag1 R2,4(8) motifs.

bind a total of 10 metal centers (two of which form the Ag1 bis-chelate unit). On the other hand, L1 acts as $\eta^{10}\mu_8$-ligand and binds eight different metal centers (two of which belong to the Ag2 unit). The sulfonate sites of L1 coordinate in different fashion: $S(1)O^{3-}$ group adopts $\eta^4\mu_4$ coordination mode, whereas $S(2)O^{3-}$ group adopts $\eta^6\mu_6$ coordination mode. Numerous catenating motifs R2,2(4), formed between the metal centers of neighboring rods, serve to interweave them into 3D coordination network (Fig. 14b). An alternative way to disentangle the crystal structure is to consider the interpenetration of two independent frameworks formed by Ag1 and Ag2 ions. The ligands L2 bridge the Ag1 ions into square grid 2D framework parallel to (*bc*) (Fig. 14c), while the ligands L1 extend the Ag2 ions into a zig-zag 1D framework along *c*-direction (Fig. 14d). The Ag2 chains interpenetrate the Ag1 layers, passing through the large windows R4,8(16), in order to interlock the neighboring layers via R2,4(8) interweaving motifs (presented on Fig. 14a). The Ag2 ions fall in the middle of the window.

Changing the meds ligand for 1,2-etds or 1,4-buds ligands in $[Ag_2(1,2\text{-etds})]_n$ **71** and $[Ag_2(1,4\text{-buds})]_n$ **72** leads to completely different organization of the crystal network. Both compounds display microporous structures. The silver ions, bonded to the

sulfonate oxygen atoms, form coordination monolayers and the alkyl spacers serve as pillars between them. However, the symmetry relationships inside the inorganic monolayers, as well as between them are different in both crystals, which results into different crystal structures. Crystal **71** is triclinic ($P\bar{1}$) and **72** is monoclinic $P2_1/c$. The inversion related sulfonate sites of 1,2-etds adopt $\eta^6\mu_6$-coordination mode in order to coordinate to six metal centers form each side of the spacer. Numerous catenating R2,2(4) motifs are used in the coordination arrays. The octahedral geometry of the silver ion in **71** is distorted by two close Ag–Ag contacts. Three different centrosymmetric R2,2(4) motifs catenate the individual coordination units in order to extend them in 2D. The metal ion in **72** is surrounded by five 1,4-buds ligands and displays a distorted trigonal bipyramidal geometry. Each of the end sulfonate site binds in $\eta^5\mu_5$ fashion five metal centers in order to extend them into 2D coordination monolayers via several R2,2(4) motifs. The closest Ag–Ag distances inside the layer are significantly longer than those in **71**. The alkyl chains arranged between the coordination layers are screw related and cross-link the monolayers in two different directions.

Compound $[Ag_2(1,5\text{-nds})]_n$ **73** is very interesting. The 1,5-nds moiety serves as $\eta^{10}\mu_8$ ligand and connects the silver ions through both Ag–sulfonate and Ag–η^2–arene interactions. The silver ions display a distorted tetrahedral geometry defined by three oxygen atoms belonging to three different sulfonate ligands and the shortest C=C bond of the naphthalene ring, which is regarded as a single donor. The packing arrangement in **73** takes place with a generation of organic and inorganic regions. The 3D coordination framework can be considered as consisting of $(0\,1\,\bar{1})$ monolayers, formed explicitly by Ag–sulfonate interactions, and ligated by Ag–η^2–arene interactions. Each sulfonate site of the aromatic spacer acts as $\eta^3\mu_3$ ligand. The Ag(I) ions are extended into 2D arrays using two linking R2,4(8) and one interweaving R3,6(12) motifs, ladder-wise propagating along the *a*-direction. The naphthalene rings inside the layer are arranged in stacks along the same direction. Big rings (with R2,4(22) motif) are encircled by the metal ions and the organic spacers (Fig. 15a). Only Ag–sulfonate interactions are used in the monolayer formation, whereas the Ag–arene interactions interlock the inversion related layers via another R2,4(12) motif in order to form porous 3D framework (shown on Fig. 15b).

8. Group 2 (earth alkaline) metal ion complexes

The main difference between the earth alkaline and the transition metal ion coordination complexes is the lack of ligand field stabilization in the former, which gives rise to irregular coordination geometries and variable coordination numbers observed in their compounds. The coordination trends of the group 2 metals can be correlated rather with the cation radius and the charge density [17]. For example, the small ionic radii and high charge density results into high affinity of magnesium ion to hard oxygen donors. Six water molecules penetrate the first coordination sphere of Mg^{2+} in compounds **31**–**33** (Table 1). The sulfonate groups do not coordinate directly to the metal ion, but form hydrogen bonds to the aqua ligands in order to extend the hydrated units into supramolecular networks. Therefore the compounds can be considered as second sphere complexes. However, the charge density decreases and the polarizability increases with growing ionic size, which allows for direct ligand

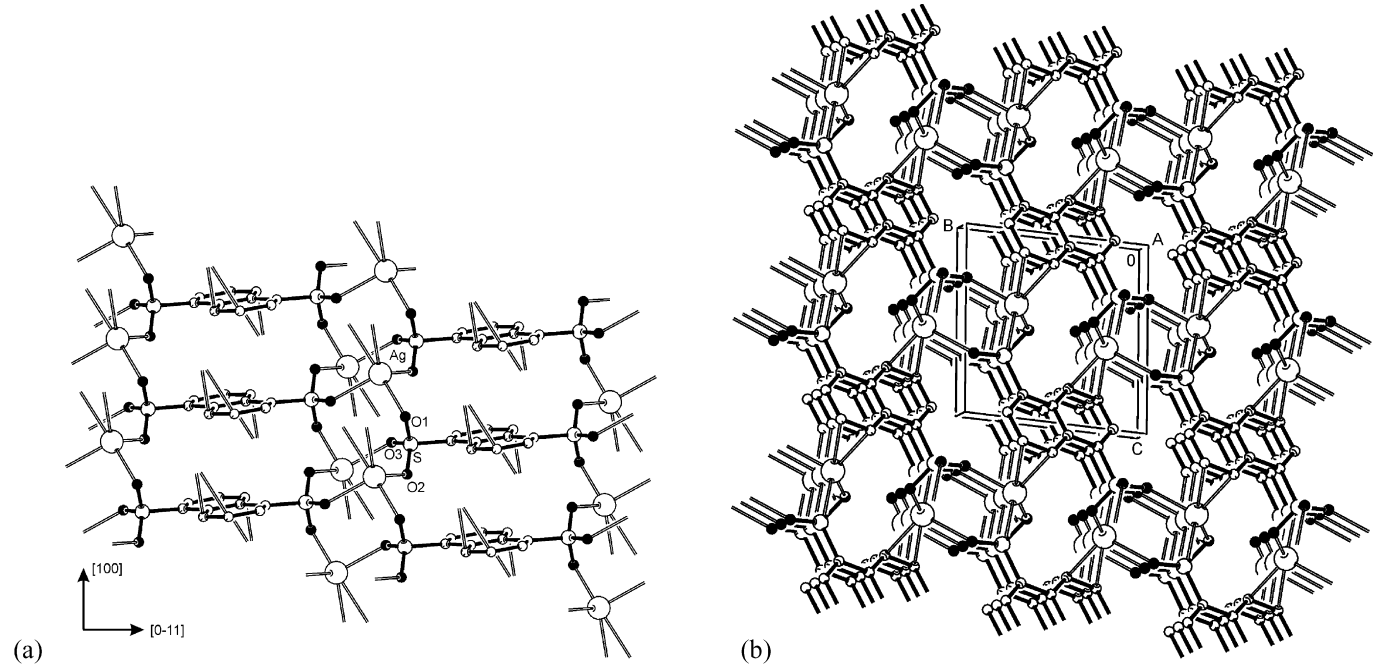

Fig. 15. The coordination monolayer $[Ag_2(1,5\text{-nds})]_n$ in **73** [Ref. 74] is formed explicitly by Ag–sulfonate interactions (a); the Ag–η^2–arene bonds join the monolayers in order to generate a porous 3D coordination framework (b).

bonding. Almost all Ca^{2+}, Ba^{2+} and Sr^{2+} disulfonates, except the aqua complexes **34**, **87** (Ca) and **81** (Ba) display extended coordination frameworks, 1D (Ca), 2D (Ca, Sr) and 3D (Sr, Ba). Chelate coordination units are readily formed with the appropriate 1,3-bds ligand (compounds **78–80**). The Ca^{2+} and Cd^{2+} form identical 2D coordination frameworks with meds and 1,5-nds ligands (compare compounds **75–77** and **82–85**). For example, the two polymorphic forms of calcium methanedisulfonate trihydrate **75**(**76**) and **77** appear to be structural isomorphs of the corresponding cadmium compounds **66** and **67** and display identical coordination networks. Hereafter, the most important coordination features of group 2 metal ions are presented and, in particular, attention is paid to their progressive trends for high-dimensional network formation.

Three crystals **78–80** are isomorphic ($P\bar{1}$) and display identical 1D coordination arrays, despite the different coordination geometry of the metal ions in them (see Table 3). The calcium ion is eight-coordinate with a square antiprism geometry and the strontium and barum ions are nine-coordinate with a tricapped trigonal bipyramid and monocapped antiprism geometry, respectively. The number of the 1,3-bds ligands in the first coordination sphere of the metal ion grows from three in Ca compound to four in Sr and six in Ba compound, whereas the number of aqua ligands drops from four to one. The 1,3-bds dianions serve as a $\eta^4\mu_3$ ligand in **78**, $\eta^5\mu_4$ in **79** and $\eta^8\mu_6$ in **80**. The *ortho*-positioned hydroxyl groups in the benzene ring favor binding to the same metal center via R1,2(5) chelate ring. The first $S(1)O_3^-$ sulfonate group serves to bridge the neighboring chelated units in order to extend them along *a*-direction via C1,2(4) motif. The 1D coordination array resembles a ladder with M^{2+} and $S(1)O_3^-$ arranged on the sidepieces and aromatic rings used as steps (see Fig. 16a). Big halls (with R2,4(16) coordination motifs) are generated between the metal ions along the array. The aromatic portions of the 1D constructions are arranged with offset-face-to-face (OFF) interactions. The aqua ligands are arranged from both sides of the ladders. The second sulfonate group $S(2)O_3^-$ (in 3-position on the ring) protrudes into the halls and serves to connect the ladders via hydrogen bonds (in **78**) and/or coordination bonds (in **79** and **80**) in order to furnish the 3D network (Figs. 16–18). Multiple aqua–sulfonate hydrogen bonds are established between the ladders in $[Ca(H_2O)_4(1,3\text{-beds})]_n{\cdot}nH_2O$ and cross-link them into 3D structure. The crystalline water is arranged in the hydrophilic channels generated between the ladders and serves to donate three hydrogen bonds toward the not coordinated (S2) site and to accept a hydrogen bond from the second hydroxyl group. The bigger ionic size of Sr^{2+} in $[Sr(H_2O)_4(1,3\text{-beds})]_n{\cdot}nH_2O$ **79** allows for a steric access to the second (S2) sulfonate group, which serves as a ninth ligand. This fact does not change the symmetry relationships along and between the ladders, but essentially changes the binding relationships between them. The S2 site in **79** binds in $\eta^1\mu_1$ fashion the strontium ion in order to interlink the neighboring ladders into two-dimensional coordination framework parallel to (*ab*) crystallographic plane (Fig. 17a). The ladder interweavement takes place via two big motifs described with R2,4(12) and R4,8(20) graphs. The hydration water resides in the interlayer region and hydrogen bonds the coordination monolayers in a 3D supramolecular network. The significant polarizability and ionic size markedly raise the metal-ligand affinity in **80**. The coordination array of the barium compound $[Ba(H_2O)(1,3\text{-beds})]_n{\cdot}nH_2O$ appears to be three-dimensional and displays a porous structure (Fig. 18a). The 1,3-beds ligand coordinates to six barium centers. The $S(1)O_3^-$ group adopts $\eta^4\mu_3$ coordination mode in order to bridge three Ba^{2+} belonging to two neighboring *y*-translated ladders. The $S(2)O_3^-$ group acts as $\eta^2\mu_2$-ligand and binds *z*-translated ladders. Therefore, the solid state organization of the compound can be considered as coordination interplay of *a*-ladders. Multiple ring motifs are used to interweave the ladders, the smallest of which R2,2(4), catenates inversion related barium centers of neighboring ladders. The structural arrangement of the compound can also be described in terms of interlocked coordination monolayers, similar to those in **79** (Fig. 18b). Numerous water–water, water–sulfonate and hydroxyl–water hydrogen bonds stabilize the network. The crystal water forms hydrogen bonded dimers $R_2^2(4)$, arranged in big chambers R4,8(16) closed between the barium centers.

The solid state organization of $[Ca_2(H_2O)_4(1,5\text{-nds})_2]_n$ **82** demonstrates a structural similarity with that of the cadmium analogue $[Cd_4(H_2O)_8(1,5\text{-nds})_4]_n$ **68** and both compounds crystallize with the same space group ($P\bar{1}$). The six coordinate Ca^{2+} is very close in size to Cd^{2+} and displays similar monolayer arrangement. The coordination modes used for formation of the Ca–Ca dimers and for their extension into ribbons are the same as in **68**. The naphthalene rings, linking the ribbons in 2D, are also inclined to the mean plane of the coordination monolayer and packed with EF interactions. However, the symmetry relationships inside the monolayers of the calcium compound are different. There is no differentiation of the metal ions and symmetry breaking of the 2D coordination array in **82**. Unlike cadmim, calcium ion does not suffer the directional demands of d-electon orbitals. Therefore, the coordination geometry of Ca^{2+} is flexible, which allows the dinuclear unit to adapt the requirements of the network. However, the preservation of the inversion relation between the sulfonate sites, as well as between the coordination ribbons is accompanied by significant deformations of the coordination octahedron in **82**.

Compounds $[Sr(H_2O)(1,5\text{-nds})]_n$ **84** and $[Ba(H_2O)(1,5\text{-nds})]_n$ **85** are isostructural, with *Pnma* space group and a pillar structure. The eight-coordinate metal ion therein is coordinated by six different 1,5-nds and two water ligands and displays a bisdisphenoidal configuration. One way to present the three-dimensional coordination array in **84** and **85** is to consider it as formed from metal ion–sulfonate coordination monolayers (similar to those in **68** and **82**), which are interlinked in the third dimension via two coordination bonds donated from the third O-atom on each sulfonate site (Fig. 19a). However, with respect to the three-dimensional connectivity patterns of the coordination array in **84** and **85**, an alternative description of the crystal organization seems to be more appropriate. Similar to **68** and **82**, the organic and inorganic portions of the compounds are arranged in regions along *b*-axis. While Ca and Cd ions in **68** and **82** are able to connect the organic portions only in two directions, the big Ba and Sr ions in **84** and **85** allow for cross-

Table 3
Group 2 (earth alkaline) metal ion complexes

Compound name/formula	Ref. code	Space group	Configuration of the coord. unit(s)/ligand binding mode(s)	Linking motif(s)/1D array(s) formed by disulfonate ligands	3D network	Reference
75. Calcium methanedisulfonate trihydrate $[Ca(H_2O)_3(meds)]_n$	CAMSOA01	$P2_1/n$	Ca–pentagonal bipyramid; meds: $\eta^4\mu_3$ ligand, bidentate bonding to form chelate ring R1,2(6)	C1,2(4) along [1 0 0], C1,2(4) along [1 0 1], R3,6(14) windows	Coordination interplay of chelate units via C1,2(4) motifs to form (*ac*) layers; Intra a. interlayer aqua-sulfonate h.b	[74]
76. Calcium methanedisulfonate trihydrate $[Ca(H_2O)_3(meds)]_n$	CAMSOA02	$P2_1/n$	Ca–pentagonal bipyramid; meds: $\eta^4\mu_3$ ligand; bidentate bonding to form R1,2(6)	C1,2(4) along [1 0 0], C1,2(4) along [1 0 1], R3,6(14) windows	Interweavement of glide related chains via C1,2(4) motifs to form (*ac*) layers; Intra a. interlayer water-sulfonate h.b	[67]
77. Calcium methanedisulfonate trihydrate $[Ca_2(H_2O)_6(meds)_2]_n$	CAMSOA	$P\bar{1}$	Ca1, Ca2–pentagonal bipyramids; two distinct $\eta^4\mu_3$ ligands forming two chelate coord. units R1,2(6)	Ca1 chains via C1,2(4), Ca2 chains via C1,2(4); two different R3,6(14)	Ca1, Ca2 chains interweaved via C1,2(4) to form (*ac*) coord. layer, intra a. interlayer water-sulfonate h.b	[68]
78. catena-((μ_3-4,5-Dihydroxybenzene-1,3-disulfonato)-tetraaqua-calcium monohydrate) $[Ca(H_2O)_4(1,3\text{-}bds)]_n{\cdot}nH_2O$	OMARAV	$P\bar{1}$	Ca–square antiprism; 1,3-bds is $\eta^4\mu_3$ligand: hydroxyl sites chelate Ca via R1,2(5); $S(1)O_3^-$: $\eta^2\mu_2$ mode to form ladder	C1,2(4) extends the chelate units into coord. ladder along *a*-axis, R2,4(16) motifs generated along the ladder.	3D hydrogen bonded network via Ow-H···O(S) hydrogen bond interactions.	[48]
79. catena((μ_4-4,5-Dihydroxybenzene-1,3-disulfonato)-tetraaqua-strontium monohydrate) $[Sr(H_2O)_4(1,3\text{-}beds)]_n{\cdot}nH_2O$	OMAREZ	$P\bar{1}$	Sr–tricapped trigonal bipyramid; 1,3-bds is $\eta^5\mu_4$ ligand: $S(1)O_3^-$: $\eta^2\mu_2$ mode to form ladder; $S(2)O_3^-$: $\eta^1\mu_1$ mode to interlink the ladders in 2D coord. network	Coord. ladders via C1,2(4), R2,4(16), ladders are interplayed via R2,4(12) and R4,8(20)	2D coordination monolayer; 3D hydrogen bonded network: intralayer O_h-H···O(S2) and Ow-H···O(S2) hydrogen bonds; interlayer water-sulfonate and hydroxyl-water h.b	[48]
80. catena-((μ_6-4,5-Dihydroxybenzene-1,3-disulfonato)-aqua-barium monohydrate) $[Ba(H_2O)(1,3\text{-}bds)]_n{\cdot}nH_2O$	HUCMOH	$P\bar{1}$	Ba-9-coord, monocapped antiprism; 3,4-hydroxyl groups: $\eta^2\mu_1$ chelate, $S(1)O_3^-$: $\eta^4\mu_3$ mode to form ladder; $S(2)O_3^-$: $\eta^2\mu_2$ mode to link the ladders	R1,2(4), R1,2(5) chelate rings, R2,2(4), R2,4(8) linking motifs; R2,4(16) and R3,6(16)	Porous 3D coordination network; 3D hydrogen bonded network	[75]
81. bis(6-Ammonionaphthalene-1,3-disulfonato)-hexa-aqua-barium tetrahydrate $[Ba(1,3\text{-}ands)_2(H_2O)_6]{\cdot}4H_2O$	NIHSIG	$C2/c$	Ba(II)–8-coordinated, antiprism, $\eta^1\mu_1$ ligands		Hydrogen bonded 3D network	[39]
82. catena-(bis(μ_4-1,5-Naphthalenedisulfonato)-tetra-aqua-di-calcium) $[Ca_2(H_2O)_4(1,5\text{-}nds)_2]_n$	RAKYUX	$P\bar{1}$	Ca–deformed octahedral, 1,5-nds: $\eta^4\mu_4$ ligands	$(1\,\bar{1}\,0)$ coord. monolayers via two R2,4(8) motifs	Interlayer water-sulfonate h. bonds, organic/inorganic regions	[47]
83. catena-((μ_6-1,5-Naphthalenedisulfonato)-diaqua-barium(ii)) $[Ba(1,5\text{-}nds)(H_2O)_2]_n$	FOBYAX	$C2/c$	Ba–square antiprism, both sulfonate sites: $\eta^3\mu_3$ ligands, aqua: $\eta^1\mu_1$ ligand	Coordination monolayers via three different R2,4(8) linking motifs	3D coordination network; the (*ab*) inorganic monolayers are pillared by organic spacer.	[76]
84. catena-((μ_6-1,5-Naphthalenedisulfonato)-(μ_2-aqua)-strontium) $[Sr(1,5\text{-}nds)(H_2O)]_n$	RAKZAE[a]	$Pnma$	Sr–bisdisphenoidal configuration; both sulfonate sites: $\eta^3\mu_3$ ligands, aqua: $\eta^2\mu_2$ ligand	Coord. monolayers via three R2,4(8) motifs; R3,6(12), R2,3(6), R3,5(10)	Pillared (*ac*) coord. monolayers; inorganic/organic regions along *b*-axis	[47]
85. catena-((μ_6-1,5-Naphthalenedisulfonato)-(μ_2-aqua)-barium) $[Ba(1,5\text{-}nds)(H_2O)]_n$	RAKZEI	$Pnma$	Ba–bisdisphenoidal configuration; both sulfonate sites: $\eta^3\mu_3$ ligands; aqua: $\eta^2\mu_2$ ligand	Coord. monolayers via three R2,4(8) motifs; R3,6(12), R2,3(6), R3,5(10)	Pillared (*ac*) coord. monolayers; inorganic/organic regions along *b*-axis	[47]
86. catena-((μ_5-Naphthalene-2,7-disulfonato)-(μ_2-aqua)-aqua-barium(ii)) $[Ba(H_2O)_2(2,7\text{-}nds)]_n$	YAFWEI	$Pna2_1$	Ba–square antiprism; 2,7-nds: $\eta^5\mu_5$ ligand; aqua ligands: $\eta^2\mu_2$ and $\eta^1\mu_1$	$S(1)O^{3-}$ group: $\eta^3\mu_3$ mode, $S(2)O^{3-}$ group: $\eta^2\mu_2$ mode; R2,3(6), R2,4(8), R3,5(22)	3D coord. network with R4,8(40) channels; coord. water is arranged in there via Ow-H···O(S2) interactions.	[77]
87. Hexa-aqua-(4-amino-4′-ammonio-5,5′-dimethyl-1,1′-biphenyl-2,2′-disulfonato-*O*)-calcium 4-amino-4′-ammonio-5,5′-dimethyl-1,1′-biphenyl-2,2′-disulfonate hexahydrate, $[Ca(H_2O)_6(2,2\text{-}ambpds)][2,2\text{-}ambpds]{\cdot}H_2O$	TEGMEX	$P\bar{1}$	Isolated coord. units, Ca(II)–intermediate between deformed pentagonal bipyramid and monocapped octahedron:		3D hydrogen bonded network; alternating inorganic–organic regions along *b*-axis	[78]
88. catena(Tetra-aqua-(4,4′-diamino-5,5′-dimethyl-1,1′-biphenyl-2,2′-disulfonato-*O*,*O*′)-calcium) $[Ca(H_2O)_6(2,2\text{-}ambpds)]_n$	TEGMAT	$P2_1/c$	$S(1)O_3^-$: $\eta^1\mu_1$ coord, mode; $S(2)O_3^-$: $\eta^2\mu_2$ coord, mode	C1,2(9) coord. chains interplayed via C2,4(8) motifs to give coord. rods along *a*-axis	Hydrogen bonded (001) monolayers via coord. water–sulfonate interactions; Interlayer hydrophobic interactions (*bc*) coord. monolayers	[78]
89. catena((μ_2-2,2′-Azino-bis(*N*-ethylbenzothiazoline-6-sulfonato))-(μ_2-aqua)-aqua-calcium) $[Ca(ABTS)(H_2O)_2]{\cdot}H_2O$	IJIDOU[b]	$C2/c$				[79]
90. catena-(bis(μ_8-1,2-Dioxy-3,5-benzenedisulfonato)-tetrakis(μ_2-aqua)-tetra-aqua-penta-sodium-manganese(iii) dihydrate)	JAFPUC	$P\bar{1}$	Mg–tetrahedral, Na1 trigonal bipyramid, Na2 trigonal antiprism, Na3 octahedral	1D Mg chains	3D coordination networks	[80]

[a] Structures assigned with asterisk are disordered.
[b] Structure omitted from the discussion (disordered sulfonate group).

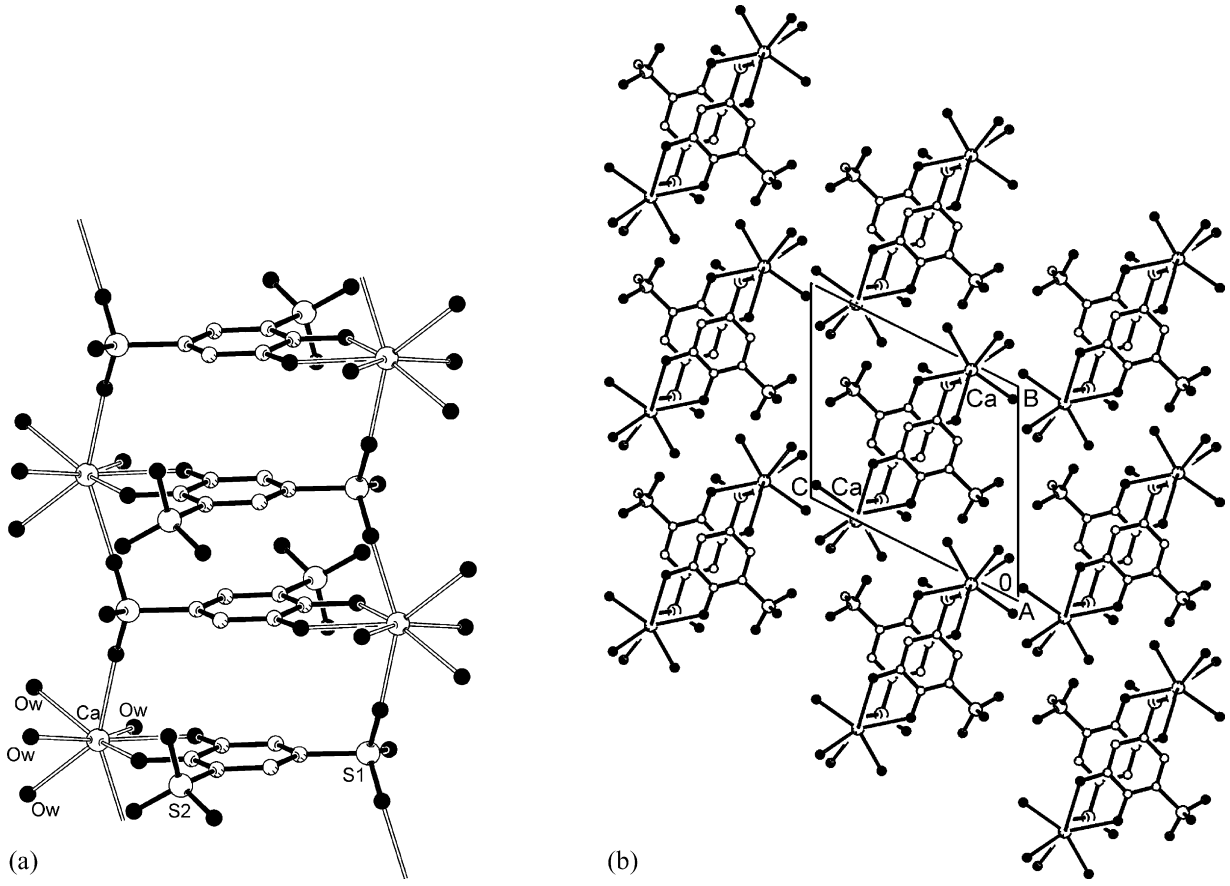

Fig. 16. (a) The ladder construction of the 1D coordination array $[Ca(H_2O)_4(1,3\text{-bds})]_n$ in crystal **78** (Ref. [48]); (b) the packing arrangement of the coordination ladders, viewed along the array. For the sake of clarity, the hydrogen atoms are omitted.

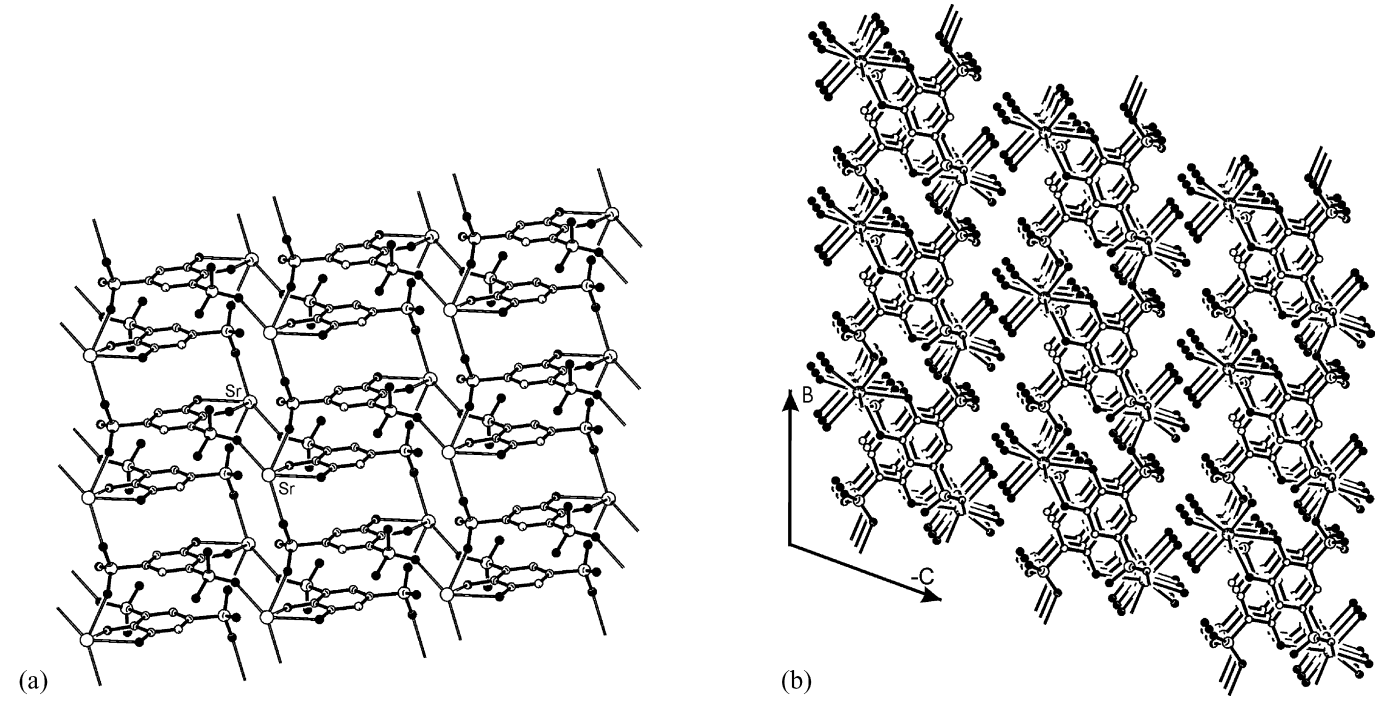

Fig. 17. (a) The 2D coordination framework $[Sr(H_2O)_4(1,3\text{-beds})]_n$ in compound **79** (Ref. [48]). The a-ladders are interweaved via R2,4(12) and R4,8(20) linking motifs in order to form (*ab*) monolayers. For the sake of clarity the aqua ligands are not shown in the picture; (b) view along the ladders presenting the relationships between three coordination monolayers. The crystalline water and the hydrogen atoms of 1,3-beds and aqua ligands are omitted from this picture.

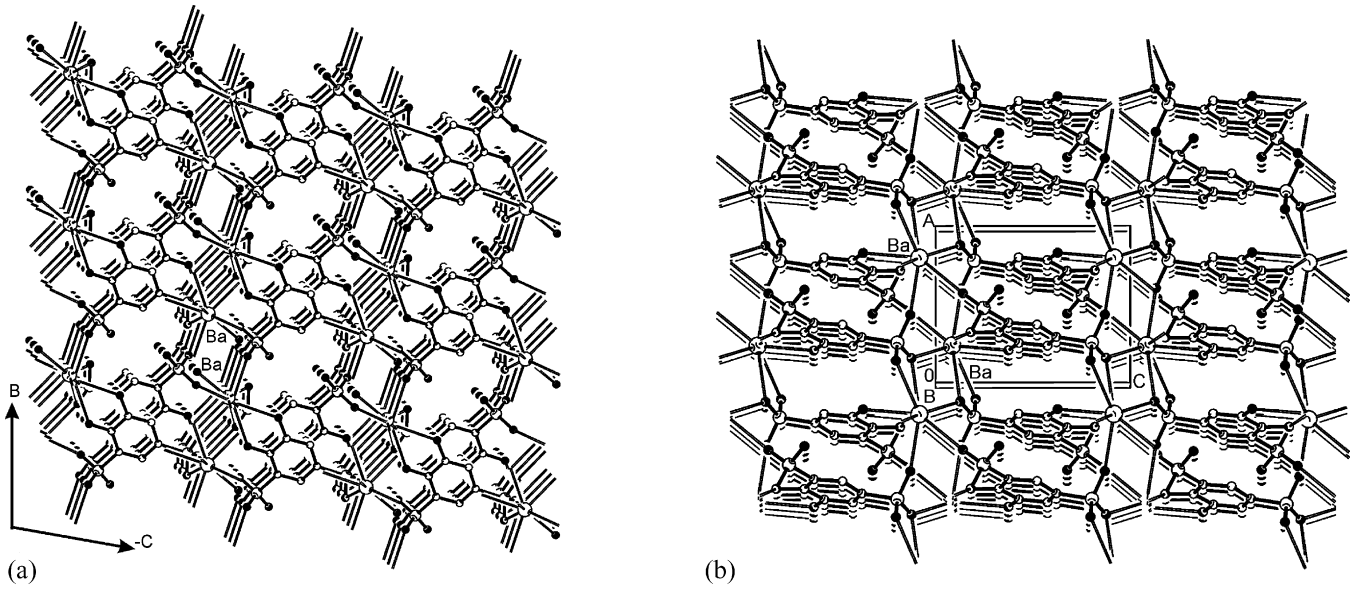

Fig. 18. (a) The *a*-ladders $[Ba(1,3\text{-beds})(H_2O)]_n$ interweave in order to form a porous 3D coordination network in crystal **80** (Ref. [75]). The hydration water molecules (not shown in the picture) are arranged in the big chambers R4,8(16), and form hydrogen bonded dimers $R_2^2(4)$; (b) The framework of the crystal can also be considered to be formed from (*ab*) coordination monolayers, interlinked via R1,2(4) and R2,2(4) coordination motifs. For the sick of clarity all hydrogen atoms and hydrogen bonds are omitted.

linking in three different directions. So, the crystals **84** and **85** can be considered to be formed from alternating organic and inorganic monolayers (Fig. 19b). The metal ions serve to connect the organic monolayers, while the organic spacers of the ligands act as pillars between the coordination monolayers. The inorganic (coordination) monolayer contains the metal ions and the sulfonate groups. The metal centers are at special position in the reflection plane and are coordinated by ligands arranged from both sides of this plane. Each sulfonate group bridges with $\eta^3\mu_3$ mode three neighboring metal ions in order to extend them into (*ac*) coordination layer. However, the six sulfonate groups, bonded to each ion, are pair-wise reflection related and each reflection related ligand pair is knotted at three metal centers via three different R2,4(8) ring motifs (Fig. 19c). Big R3,6(12) ring motifs, are generated in the coordination monolayers. The aqua ligand bridges, in $\eta^2\mu_2$ fashion, the neighboring metal centers along the *a*-axis, which is accompanied by generation of two more R2,3(6) and R3,5(10) motifs (see Fig. 19c). The naphthalene rings of the organic layers align along *c*-axis with EF interactions between them. Compound **83** $[Ba(H_2O)(1,5\text{-nds})]_n$ (*C*2/*c*), also displays a pillared structure, however both the coordination geometry and the arrangement of the barium ions inside the inorganic monolayer are quite different from those in crystal **85** (compare Fig. 19c and d). Unlike the former two crystals the crystal network in **83** cannot be disentangled into formal barium sulfonate monolayers.

The symmetry of the nds-ligands is dependent upon the topology of the coordination sites. While the sulfonate groups are symmetrically arranged versus the middle point of C9=C10 bond in 1,5-nds and 2,6-nds, they are symmetric versus the line of C9=C10 bond in 2,7-nds ligand (see Scheme 3). On the other hand the symmetry relationships in the crystal depend on the symmetry of the basic units and their arrangement in the network. The lack of an inversion center in the building block is the first and the most important requirement for polar design and any task for polar alignment of centrosymmetric units will obviously fail. However, in praxis, it is difficult to eliminate the predominance of the dipole–dipole interactions unless additional structure controlling factors and/or competing bonding interactions are introduced. A good demonstration of the above considerations is compound $[Ba(H_2O)_2(2,7\text{-nds})]_n$ **86**, which crystallizes with the noncentrosymmetric $Pna2_1$ space group. The central ion displays a square antiprism geometry with five 2,7-nds and three aqua ligands (two of which are shared between neighboring centers). Two monodentate Ba–O(S1) and Ba–O(S2) bonds, donated from both sulfonate sites are used to extend the barium centers into C1,2(10) sinusoidal arrays along the *b*-direction. The lack of inversion center imposed on the ligand spacer allows for a polar alignment along the chains. Parallel chains link (via another Ba–S(2) bond) into a wavy coordination monolayer with big hollows (described with R3,6(24)) encircled by three barium ions and three 2,7-nds ligands. The aqua ligand also bridges in $\eta^2\mu_2$ fashion the neighboring chains of the monolayer generating two additional linking motifs R2,3(6) and R3,5(22) (see Fig. 20a). On the other hand, the S(1) site acts as $\eta^3\mu_3$ ligand and serves to interweave (via an R3,6(12) motif) the metal ions belonging to three different monolayers. Two different R2,4(8) motifs, alternating along the *a*-axis are used to interplay the neighboring monolayers (Fig. 20b). The non-coordinated oxygen atom of the S2 site and the second $(\eta^1\mu_1)$ aqua ligand are arranged in the big R4,8(40) channels generated between the monolayers. Three hydrogen bonds, donated from the water molecules toward the non-coordinated oxygen atom, additionally cross-link the monolayers furnish-

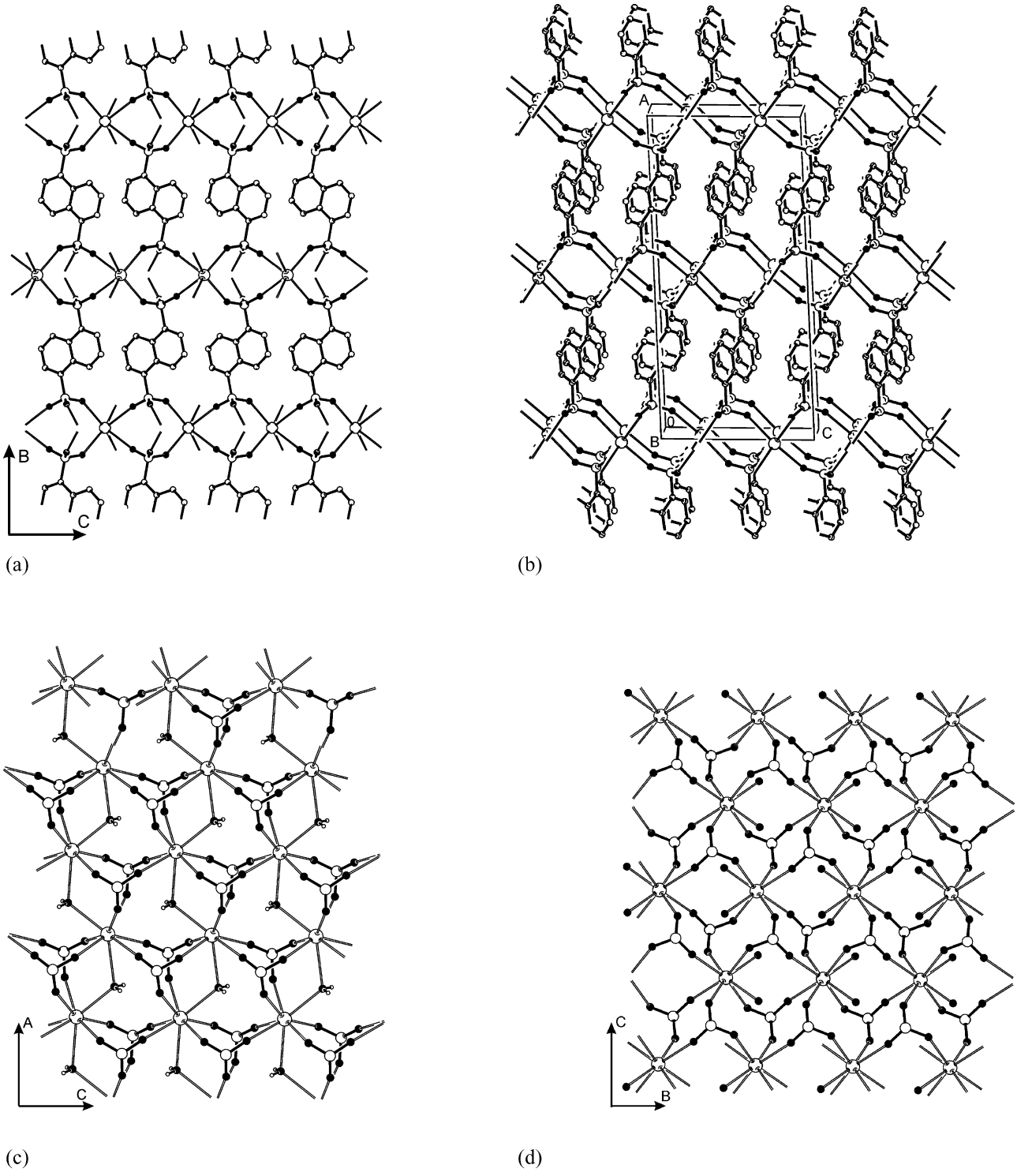

Fig. 19. The crystal structure in crystals **84** and **85** (Ref. [47]) can be considered as: (a) parallel arrangement of 2D coordination networks, interlocked in the third direction; (b) formed from inorganic coordination monolayers pillared by the organic spacers. The aqua ligand and the hydrogen atoms on the aromatic rings are omitted from pictures (a) and (b). View of the coordination monolayers in crystals **84** and **85** (c) and **83** (Ref. [76]) (d). For the sake of clarity the aromatic rings of 1,5-nds ligands and the hydrogen atoms of the aqua ligands (in **83**) are omitted from pictures (c) and (d).

ing the final 3D coordination and supramolecular network of the compound. For comparison reasons with the former compounds, one can consider that the barium ions and the aromatic portions are arranged in alternating (1 1 0) inorganic and organic monolayers. However, the symmetry requirements of the 3D networks cause the naphthalene rings to somewhat penetrate the inorganic monolayers and there is no clear separation between them.

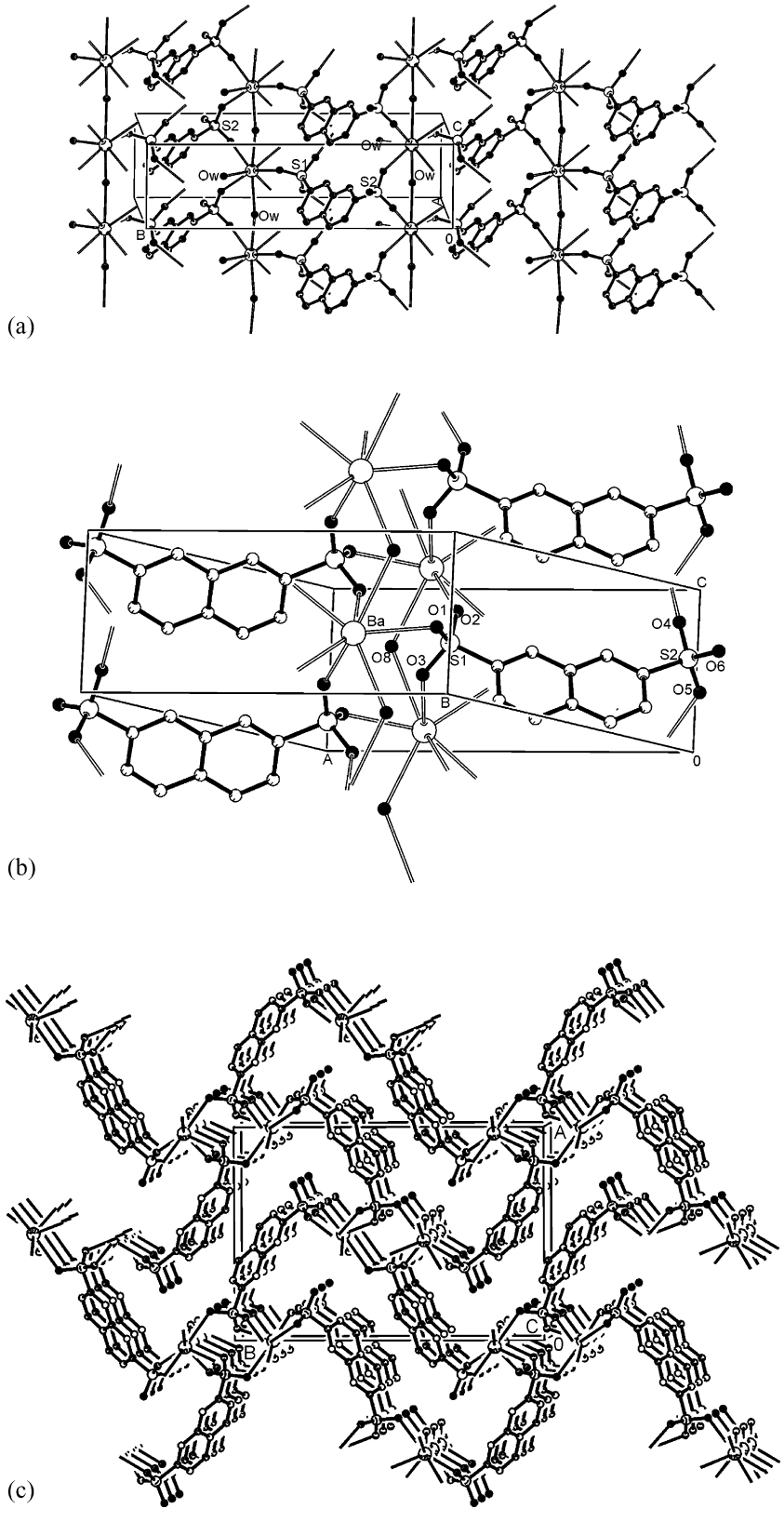

Fig. 20. (a) View of the wavy monolayer in $[Ba(2,7\text{-nds})(H_2O)_2]_n$ **86** (Ref. [77]). Two coordination motifs R2,3(6) and R3,5(22) are generated therein; (b) Presentation of the R2,4(8), R3,6(12) and R4,8(16) motifs responsible for the 3D coordination interplay. (c) View along the undulate monolayers showing the R2,4(8) ring motifs used to interlink the monolayers and the big R4,8(40) channels generated between the monolayers. The hydrogen bonds are omitted for clarity.

9. Summary and conclusions

Variable metal-organodisulfonate structures have been presented in the above overview and considered with respect to the increased dimensionality of the coordination networks. The key role of structure determining factors like charge, coordination predisposition, and geometrical preferences of the metal ion, on the one hand, and different coordinating abilities of the ligand(s), on the other, have been discussed throughout the paper. Structural modifications introduced by the auxiliary ligand(s) have also been shown. It is obvious that the most prominent feature of the polymer structures presented is the ability of the disulfonate anion to bridge between the metal centers. The presence of two functional groups linked by an appropriate spacer facilitates the extension of the metal centers at least in one direction. The shape of the electron density around the sulfonate group (see Scheme 1) allows one to design structures with increased connectivity of the metal-ligand network. The orientational freedom of the ligand lone pairs is reduced by the rigidity of the spacer.

However, the organic disulfonates possess relatively soft basic properties, and therefore, the dimensionality of the coordination framework depends upon the chemical nature of the metal and its coordination geometry. For that reason hard transition metal ions like Co^{3+}, Fe^{3+} and the small Mg^{2+} ion preferentially form isolated aqua units without direct or with a single coordination bond to the sulfonate moiety (compounds **1–39** in Table 1 and **42–50** in Table 2). The coordination geometry and the nuclearity of these units are strongly dependent upon the geometry of the ligands in the first coordination sphere, and upon the topology and the stereo accessibility of their donors. The metal ions in compounds **51–65** (Cu^{2+}, Sn^{2+}, Ni^{2+}) lie at the border line of hard/soft transition metals and are bound with $\eta^1\mu_1$ coordination mode in order to form chains C1,2(*n*), where *n* depends upon the length of the disulfonate spacer (Table 2). However, soft transition metal ions, as well as the big earth alkaline ions (Ba^{2+}, Sr^{2+}), readily form high-dimensional coordination networks with disulfonate ligands incorporated in the first coordination sphere. A potential problem with these metal ions is, however, that they often do not impose as strong a preference for a given geometry as do other ions and this can lead to lack of predictability over the structure of the network. The disulfonate ligands penetrate the first coordination sphere of d^{10} metal ions (Ag^{1+}, Cd^{2+}) in order to form layered or porous architectures. So, 1D (Cu^{2+}, Ni^{2+}, Cd^{2+}, Ca^{2+}), 2D (Cd^{2+}, Ca^{2+}, Sr^{2+}) and 3D (Ag^{1+}, Sr^{2+}, Ba^{2+}) metal-disulfonate coordination frameworks have been found. Chelate coordination units are readily formed with an appropriate disulfonate ligand (compounds **42**, **66**, **67**, **70**, **78–81**). Both Ca^{2+} and Cd^{2+} form identical 2D coordination frameworks with meds and 1,5-nds ligands (compounds **66–68** and **79–81**).

Apart from the most prominent feature of the disulfonate anions to act as bridging ligands, their volume and shape, which must be accommodated in the crystal lattice, are also important in determining the polymer structures. Factors accounting for the coordination modes of the ligand, and therefore, for the dimensionality of the network include the geometry of the disulfonate spacer and the topology of the coordination sites. The monodentate binding mode is predominant in the majority of the compounds reviewed. However, arenedisulfonates with sulfonate (and/or other donor groups) *ortho*- or *meta*-positioned on the aromatic spacer (compounds **42**, **78–80**, **81**) as well as alkanedisulfonates with both sulfonate groups substituted at the same C-atom of the chain (methanedisulfonate in **66–67**, **70**, **75–77**) are geometrically predisposed for bidentate or bis-bidenate (**70**) binding to the metal ion. Diverse coordination modes are observed in their solid state structures starting from $\eta^4\mu_3$, $\eta^4\mu_4$ found in the cadmium complexes up to $\eta^{10}\mu_8$, $\eta^{12}\mu_{10}$, $\eta^{12}\mu_{12}$ found in five and six-coordinate Ag^+ complexes. The symmetry of the coordination polymer, to a great extent, depends on the symmetry of the spacer between the sulfonate sites (**51**, **70**) and relies on the adaptability of the coordination units (compare crystals **68** and **82**). The formation of a non-centrosymmetric coordination array and the polar crystal arrangement in compound **86** is determined by the lack of inversion center in 2,7-nds ligand, when compared to the centrosymmetric arrays in compounds with 1,5-nds and 2,6-nds ligands (**73**, **55–57**, **83–85** and **58–61**. Both 1,5-nds and 2,7-nds compounds can form 1D, 2D and 3D coordination networks, whereas only 1D arrays are observed in 2,6-nds compounds. This experimental fact may be explained by the serious packing problems faced by the 2,6-nds moiety used as $\eta^4\mu_4$ and especially $\eta^6\mu_6$ ligand. The graph describing the distance between the metal centers of the coordination array is C1,2(9) for $[M(1,5\text{-nds})]_n$ and C1,2(10) for $[M(2,7\text{-nds})]_n$. The shortest path in $[M(1,5\text{-nds})]_n$ goes through the C9–C10 bond. However, compounds $[M(2,6\text{-nds})]_n$ are characterized with C1,2(11), no matter which path is used. An '11 bond' distance seems to be too long for an efficient 2D coordination interplay.

Finally, recurring coordination motifs are found in the dimer and multimer coordination units, and their polymer extensions. The most abundant motifs are the intertwining R2,4(8) motif, and the catenating R2,2(4) motif. The analogy between the coordination ring motif, described with R2,4(8) and the corresponding hydrogen bonded ring motif $R_2^2(8)$ is evident. Each of them presents the same graph and describes the structural relationships between two metal/hydrogen atoms in the eight-member cycle dimer. The same number of electrons are incorporated in the formation of the ring and the different formal notations of the graph reflect the different character of the connections (bonds). Eight-member rings are widespread as linking motifs for the formation of robust coordination and supramolecular networks. Bigger ring motifs R3,6(12), R4,8(16) also have corresponding analogues in the extended hydrogen bonded networks (see Scheme 2). Therefore, it seems reasonable to consider the coordination motifs, recurrent in different structures, as coordination synthons relevant to the supramolecular synthons, broadly used in crystal engineering. One can believe that this approach may be applicable for the design of new structurally based materials.

Acknowledgement

Financial support from Wroclaw University of Technology (Project Grant) is thankfully acknowledged.

Appendix A

All abbreviations used throughout this paper are summarized as follows:

1. The disulfonate ligands are assigned as

meds methanedisulfonate
1,2-etds ethane-1,2-disulfonate
1,4-buds buthane-1,4-disulfonate
1,2-bds 1,2-benzenedisulfonate
1,3-bds 4,5-dihydroxybenzene-1,3-disulfonate
1,3-ands 6-aminonaphthalene-1,3-disulfonate
2,6-ipds 4-chloro-2,6-disulfono-
methyl(imino)methyl)phenol
1,5nds 1,5-naphtalenedisulfonate
2,6-nds 2,6-naphthalenedisulfonate
2,7-nds 2,7-naphthalenedisulfonate
ABTS 2,2-azino-bisN-ethylbenzothiazoline-6-sulfonate
2,2-ambpds 4,4′-diamino-5,5′-dimethyl-1,1′-biphenyl-
2,2′-disulfonate

2. The auxiliary ligands are assigned as

peds 4,4′-phenyletherdisulfonate
bpds 4,4′-biphenyldisulfonate
2,2′-bpy 2,2′-bipyridyl
en ethylenediamine
N-meen *N*-methylenediamine
N,*N*′-meen *N*,*N*′-dimethylenediamine
4-cyclam 1,4,8,11-tetraazacyclotetradecane
5-cyclam 13-methyl-6-(1-phenylethyl)-1,4,6,8,11-
pentaazacyclotetradecane
inia isonicotinamide
pn 2,3-diaminopropane
phen phenanthroline.

References

[1] J.M. Lehn, Angew. Chem. Int. Ed. Engl. 29 (1990) 1304.
[2] D. Braga, Chem. Commun. (2003) 2751.
[3] J.D. Dunitz, Pure Appl. Chem. 63 (1991) 177.
[4] M.J. Zaworotko, Chem. Commun. (2001) 1.
[5] G.R. Desiraju, Angew. Chem. Int. Ed. Engl. 34 (1995) 2311.
[6] S.R. Batten, R. Robson, Angew. Chem. Int. Ed. Engl. 37 (1998) 1460.
[7] B.F. Abrahams, B.F. Hoskins, R. Robson, J. Am. Chem. Soc. 113 (1991) 3606.
[8] L. Carlucci, G. Ciani, D. Prosperio, Coord. Chem. Rev. 246 (2003) 247.
[9] E. Matczak-Jon, V. Videnova-Adrabinska, Coord. Chem. Rev. 249 (2005) 2458.
[10] V.A. Russel, M.C. Etter, M.D. Ward, Chem. Mater. 6 (1994) 1206.
[11] V.A. Russel, M.C. Etter, M.D. Ward, J. Am. Chem. Soc. 116 (1994) 1941.
[12] V.A. Russel, M.D. Ward, Chem. Mater. 9 (1997) 1123.
[13] J.A. Swift, A.M. Reynolds, M.D. Ward, Chem. Mater. 10 (1998) 4159.
[14] J.A. Swift, M.D. Ward, Chem. Mater. 12 (2000) 1501.
[15] M.J. Horner, K.T. Holman, M.D. Ward, Angew. Chem. Int. Ed. Engl. 40 (2001) 4045.
[16] R. Custelcean, M.D. Ward, Angew. Chem. Int. Ed. Engl. 41 (2002) 1724.
[17] A.P. Côté, G.K.H. Shimazu, Coord. Chem. Rev. 245 (2003) 49.
[18] F.H. Allen, W.D.S. Motherwell, Acta Crystallogr. Sect. B58 (2002) 380.
[19] V.A. Russel, C.C. Evans, Wenjie Li, M.D. Ward, Science 276 (1997) 575.
[20] C.C. Evans, L. Sukarto, M.D. Ward, J. Am. Chem. Soc. 121 (1999) 320.
[21] K.T. Holman, M.D. Ward, Angew. Chem. Int. Ed. Engl. 439 (2000) 1653.
[22] A.M. Pivovar, K.T. Holman, M.D. Ward, Chem. Mater. 13 (2001) 3018.
[23] J.A. Swift, A.M. Pivovar, A.M. Reynolds, M.D. Ward, J. Am. Chem. Soc. 120 (1998) 5887.
[24] K.T. Holman, S.M. Martin, D.P. Parker, M.D. Ward, J. Am. Chem. Soc. 123 (2001) 4421.
[25] K.T. Holman, A.M. Pivovar, M.D. Ward, Science 294 (2001) 1907.
[26] J. Cai, Coord. Chem. Rev. 248 (2004) 1061.
[27] M.C. Etter, J. McDonald, J. Bernstein, Acta Crystallogr. B46 (1990) 256.
For the sake of clarity, the alternative notation $R_d^a(n)$ is used throughout this paper for characterizing the hydrogen bonded ring motifs: *a*—number of hydrogen bond acceptors (proton acceptors), *d*—number of hydrogen bond donors (proton donors), *n*—number of atoms in the ring. For more details on graph-set notation of hydrogen bonds see M.C. Etter, Acc. Chem. Res. 23 (1990) 120.
[28] J. Cai, X.-P. Hu, J. Feng, X.-L. Feng, Conference (2002) 361.
[29] W.D. Harrison, B.J. Hathaway, D. Kennedy, Acta Crystallogr. Sect. B 35 (1979) 2301.
[30] S. Gao, Li-H. Huo, H. Zhao, S.W. Ng, Acta Crystallogr. Sect. E 61 (2005) m285.
[31] Li-H. Huo, S. Gao, S. Xu, H. Zhao, Acta Crystallogr. Sect. E 61 (2005) m449.
[32] W.-G. Wang, J. Zhang, Z.-F. Ju, L.-J. Song, Appl. Organomet. Chem. 19 (2005) 191.
[33] I.M. Atkinson, F.R. Keene, J.M. Gulbis, G.H. Searle, E.R.T. Tiekink, J. Mol. Struct. 265 (1992) 189.
[34] D.-L. An, S. Gao, Z.-B. Zhu, L.-H. Huo, H. Zhao, Acta Crystallogr. Sect. E 60 (2004) m111.
[35] D.S. Reddy, S. Duncan, G.K.H. Shimizu, Angew. Chem. Int. Ed. 42 (2003) 1360.
[36] C.-H. Chen, J. Cai, X.-L. Feng, X.-M. Chen, J. Chem. Cryst. 31 (2001) 271.
[37] N. Ohata, H. Masuda, O. Yamauchi, Inorg. Chim. Acta 300 (2000) 749.
[38] C.-H. Chen, J. Cai, X.-L. Feng, X.-M. Chen, Polyhedron 21 (2002) 689.
[39] A. Neels, B.M. Neels, H. Stoeckli-Evans, A. Clearfield, D.M. Poojary, Inorg. Chem. 37 (1997) 3402.
[40] B.J. Gunderman, I.D. Kabell, P.J. Squattrito, S.N. Dubey, Inorg. Chim. Acta 258 (1997) 237.
[41] J. Cai, X.-L. Feng, X.-P. Hu, Acta Crystallogr. Sect. C 57 (2001) 116.
[42] C.T. Abrahams, R. Blackshaw, G.B. Deacon, B.M. Gatehouse, G. Henkel, R. Herkelmann, R. Juschke, A. Philosof, P. Rieland, P. Sartori, Z. Anorg. Allg. Chem. 626 (2000) 2012.
[43] J.-W. Cai, C.-H. Chen, J.-S. Zhou, Chin. J. Inorg. Chem. 19 (2003) 81.
[44] C.-H. Chen, J.-W. Cai, X.-L. Feng, X.-M. Chen, Chin. J. Inorg. Chem. 18 (2002) 659.
[45] J. Cai, C.-H. Chen, C.-Z. Liao, J.-H. Yao, X.-P. Hu, X.-M. Chen, J. Chem. Soc. Dalton Trans. (2001) 1137.
[46] L.-H. Huo, S. Gao, Z.-Z. Lu, S.-X. Xu, H. Zhao, Acta Crystallogr. Sect. E 60 (2004) m1205.
[47] J. Cai, C.-H. Chen, C.-Z. Liao, X.-L. Feng, X.-M. Chen, Acta Crystallogr. Sect. B 57 (2001) 520.
[48] A.P. Côté, G.K.H. Shimizu, Chem. Eur. J. 9 (2003) 5361.
[49] W.H. Ojala, L.K. Lu, K.E. Albers, W.B. Gleason, T.I. Richardson, R.E. Lovrien, E.A. Sudbeck, Acta Crystallogr. Sect. B 50 (1994) 684.
[50] C. Piguet, G. Bernardinelli, A.F. Williams, Inorg. Chem. 28 (1989) 2920.
[51] C.-H. Chen, J. Cai, X.-M. Chen, Acta Crystallogr. Sect. C 58 (2002) m59.
[52] A. Neels, B.M. Neels, H. Stoeckli-Evans, A. Clearfield, D.M. Poojary, Inorg. Chem. 36 (1997) 3402.
[53] J. Cai, X.-P. Hu, J.-H. Yao, L.-N. Ji, Inorg. Chem. Commun. 4 (2001) 478.
[54] P.M. Forster, M.M. Tafoya, A.K. Cheetham, J. Phys. Chem. Solids 65 (2004) 11.
[55] N. Usuki, M. Ohba, H. Okawa, Bull. Chem. Soc. Jpn. 75 (2002) 1693.
[56] Z.-B. Zhu, S. Gao, L.-H. Huo, S.W. Ng, Acta Crystallogr. Sect. E 61 (2005) m288.
[57] T.M. Cocker, R.E. Bachman, Chem. Commun. (1999) 875.

[58] C.-H. Chen, J. Cai, C.-Z. Liao, X.-L. Feng, X.-M. Chen, S.W. Ng, Inorg. Chem. 41 (2002) 4967.
[59] V. Chandrasekhar, R. Boomishankar, A. Steiner, J.F. Bickley, Organometallics 22 (2003) 3342.
[60] J. Hausmann, S. Kass, S. Klod, E. Kleinpeter, B. Kersting, Eur. J. Inorg. Chem. (2004) 4402.
[61] P. Guerriero, D. Ajo, P.A. Vigato, U. Casellato, P. Zanello, R. Graziani, Inorg. Chim. Acta 141 (1988) 103.
[62] P.V. Bernhardt, T.E. Dyahningtyas, S.C. Han, J.M. Harrowfield, I.C. Kim, Y. Kim, G.A. Koutsantonis, E. Rukmini, P. Thuery, Polyhedron 23 (2004) 869.
[63] F. Charbonnier, R. Faure, H. Loiseleur, Acta Crystallogr. Sect. B. 33 (1977) 3342.
[64] F. Charbonnier, R. Faure, H. Loiseleur, Acta Crystallogr. Sect. B 33 (1977) 3759.
[65] J. Cai, C.-H. Chen, X.-L. Feng, C.-Z. Liao, X.-M. Chen, J. Chem. Soc. Dalton Trans. (2001) 2370.
[66] S. Gao, L.-H. Huo, Z.-B. Zhu, S.W. Ng, Acta Crystallogr. Sect. E 61 (2005) m476.
[67] R.E. Marsh, Acta Crystallogr. Sect. B 51 (1995) 897.
[68] F. Charbonnier, R. Faure, H. Loiseleur, Rev. Chim. Miner. 16 (1979) 555.
[69] S.-M. Ying, J.-G. Mao, Eur. J. Inorg. Chem. (2004) 1270.
[70] F. Charbonnier, R. Faure, H. Loiseleur, Acta Crystallogr. Sect. B 35 (1979) 1773.
[71] F. Charbonnier, R. Faure, H. Loiseleur, Acta Crystallogr. Sect. B 37 (1981) 822.
[72] S. Gao, Z.-Z. Lu, L.-H. Huo, Z.-B. Zhu, H. Zhao, Acta Crystallogr. Sect. C 61 (2005) m22.
[73] J. Suzuki, T. Yamauchi, H. Akashi, Bull. Res. Inst. Nat. Sci. Okayama Univ. Sci. (2001) 13.
[74] A. Karipides, Acta Crystallogr. Sect. B 37 (1981) 2232.
[75] A.P. Côté, G.K.H. Shimizu, Chem. Commun. (2001) 251.
[76] S. Gao, Z.-B. Zhu, L.-H. Huo, S.W. Ng, Acta Crystallogr. Sect. E 61 (2005) m528.
[77] L.-H. Huo, S. Gao, S.-X. Xu, H. Zhao, S.W. Ng, Acta Crystallogr. Sect. E 60 (2004) m1240.
[78] B.J. Gunderman, P.J. Squattrito, Acta Crystallogr. Sect. C. 52 (1996) 189.
[79] A. Denis, P. Palvadeau, P. Molinie, O. Chauvet, K. Boubekeur, Solid State Sci. 3 (2001) 715.
[80] T.S. Sheriff, P. Carr, B. Piggott, Inorg. Chim. Acta 348 (2003) 115.